REPUBLIC OF TÜRKİYE

ALTINBAŞ UNIVERSITY

Institute of Graduate Studies

Mechanical Engineering

STUDY AND ANALYSIS OF TWO-PHASE FLOW IN AN EVAPORATOR COOLING LOOP OF A TELECOMMUNICATION SATELLITE

Fadhil SHAKIR OUDAH AL SHARHAN

Master's Thesis

Supervisor

Asst. Prof. Dr. Yaser ALAIWI

Istanbul, 2023

STUDY AND ANALYSIS OF TWO-PHASE FLOW IN AN EVAPORATOR COOLING LOOP OF A TELECOMMUNICATION SATELLITE

Fadhil SHAKIR OUDAH AL SHARHAN

Mechanical Engineering

Master's Thesis

ALTINBAŞ UNIVERSITY

2023

The thesis/dissertation titled Study and Analysis od a Two-Phase Flow in an Evaporator Cooling Loop of a Telecommunication Satellite prepared by FADHIL SHAKIR OUDAH ALSHARAN and submitted on 8/8/2023 has been **accepted unanimously/by majority of votes** for the degree of MBA/Master of Science Mechanical Engineering

Asst. Prof. Dr. Yaser ALAIWIthe
Supervisor

Thesis Defense Committee Members:

Asst. Prof. Dr. Yaser ALAIWI	Department of Mechanical Engineering, Altinbas University	
Asst. Prof. Dr. Abdullahi Abdu IBRAHIM	Department of Electrical and Computer Engineering Altinbas University	
Asst. Prof. Dr. Ahmed SADIK	Department of Mechanical Engineering Hasan Kalyoncu University	

I hereby declare that this thesis/dissertation meets all format and submission requirements of a …… (Master's/PhD) thesis/dissertation.

Submission date of the thesis to Institute of Graduate Studies:____/___/____

I hereby declare that all information/data presented in this graduation project has been obtained in full accordance with academic rules and ethical conduct. I also declare all unoriginal materials and conclusions have been cited in the text and all references mentioned in the Reference List have been cited in the text, and vice versa as required by the abovementioned rules and conduct.

Fadhil SHAKIR OUDAH AL SHARHAN

Signature

DEDICATION

I would like to thank my supervisor Asst. Prof. Dr. Yaser ALAIWI, I wish to thank me committee members. I also appreciate all the support I received from my family and friends.

PREFACE

I might want to thank my administrator: Asst. Prof. Dr. Yaser ALAIWI Please let me express.

my profound feeling of appreciation and gratefulness to both of you for the information:

direction and unrestricted help you have given me. I want you to enjoy all that life has to offer.

and further achievements and accomplishments throughout your life.

ABSTRACT

STUDY AND ANALYSIS OF TWO-PHASE FLOW IN AN EVAPORATOR COOLING LOOP OF A TELECOMMUNICATION SATELLITE

AL SHARHAN, Fadhil Shakir Oudah

M.Sc., Mechincal Engineering, Altınbaş University,

Supervisor: Asst. Prof. Dr. Yaser ALAIWI

Date:August / 2023

Pages: 56

Satellites are constituted of electronic components that release heat flux. The heat released must be evacuated otherwise there are some risks to damage components in the satellite. In order to guarantee the correct working of the satellite, a thermal loop crossed by a refrigerant fluid must be added. The loop is constituted by a heater, a pressure regulator, a condenser, and a pump. The evaporator is the element of the loop in which the heat released by the electronic components is transferred to the fluid. The fluid, receiver of the components entailed energy will then be heated and will evaporate itself little by little. This breeds the appearance of a two-phase flow. An approach, developed will take into account the different models of two-phase flow that we can consider in our case. We will then be able to follow the evolution of the physical variables which characterize the system like the component temperature, the drop loss, void fraction and the quality. So, this study will provide a visualization of the thermo-hydraulics phenomenon in the evaporator, in the domain of specifications.

Keywords: Evaporator,Two-Phase Flow, Heat Transfer, Micro-Gravity, Thermosyphons (TS).

TABLE OF CONTENTS

Pages

LIST OF TABLES

Pages

LIST OF FIGURES

Pages

ABBREVIATIONS

CV2X	:	Cellular V2X
D2D	:	Device-to-Device
CNN	:	Convolutional Neural Network
OFDMA	:	Orthogonal Frequency-Division Multiple Access
RL	:	Reinforcement Learning
V2V	:	Vehicle-to-Vehicle
V2X	:	Vehicle-to-Everything

1. INTRODUCTION

The steady mission for development in heat move answers for ever-more modest and all the more impressive gadgets is driving examination toward new advancements fit for dispersing more power in less space while keeping up with high dependability prerequisites. Warm administration research has been pushed toward the improvement of another age of methods in view of two-stage advances to meet severe prerequisites of conservativeness and high intensity transitions, to accomplish successful, solid, and modest intensity move in brutal conditions like space. These advantages are acknowledged by a significant degree expansion in heat move coefficient accomplished with stream bubbling and buildup over single stage frameworks [1].

The basic role of warm administration in space applications is to keep temperatures of a sensor, part, instrument, spaceship, or space offices inside satisfactory reaches, no matter what the outer climate or warm loads forced by exercises. Objects inside the Space Transport regularly have gravity levels going from 102 to 105 g. The gravity level for the Worldwide Space Station would be somewhere in the range of 103 and 106 g. electronic chips require viable intensity departure to guarantee their constancy and forestall untimely harm. Heat dispersal in very little parts (like microelectronics) is hard to perform utilizing standard cooling strategies. Given the pattern of late years, the intricacy of the cooling framework will extend because of progressions in hardware. With the rising size of chamber stages for future review trips, huge measures of energy should be scattered or moved under gravity settings totally not quite the same as Earth, with essentially no upkeep allowed. A decrease in the quantity of moving mechanical parts becomes principal [2].

Heat Lines (HP) and Thermosyphons (TS) are two-stage inactive gadgets that utilize both reasonable and inert intensity to latently communicate heat from an intensity source to an intensity sink. They have been broadly utilized on account of their shown capacity to fulfill run of the mill measures of intense center development dispersal in numerous electronic-related applications with no outer exertion and no moving parts. In light of the real cycles included, HPs and TSs have shown astounding endpoints under the serious circumstances experienced in little devices (e.g., new ages of Ultrabooks, cell phones) and non-gravity upheld structures. (for example satellites, shuttles). In the last part of the 1990s, another age of gadgets known as Throbbing Intensity Lines (PHPs) or Wavering Intensity Lines (OHPs)

were acquainted with extend the area of materialness of two-stage uninvolved frameworks and keep awake with Warm Administration assumptions and prerequisites. PHPs are the last wilderness of two-stage inactive intensity move gadgets. PHPs could address an original elective cooling framework sooner rather than later, both for ground and space applications, in light of the fact that to their simplicity of production, ability to disseminate heat even in microgravity, and high intensity move capacities [3].

In spite of the overflow of information open in the writing (strain and temperature patterns, stream perception), there is a shortage of significant associations, robotic and computational models. In view of the different peculiarities included, PHP innovation is still distant from industrialization. PHPs are essentially founded on stage change peculiarities and slender powers; smooth movement is intrinsically non-fixed and turbulent, making getting it and demonstrating troublesome. The unmistakable Taylor stream, otherwise called slug/plug stream, is respected the underpinning of the gadget's legitimate activity, yet it is as yet hazy which boundaries signal the progress to an alternate stream design, restricting generally speaking liquid course and subsequently warm execution and application.

Two-stage detached heat move gadgets have a great many applications, including laser diodes, photovoltaic cells, and infrared finders. Various exercises have been proposed lately, yet numerous fundamental worries stay unanswered to accomplish the assembling stage and full space accreditation. Among the significant issues, a basic comprehension of the impacts of stream design changes (under differing limit conditions and intensity loads) on nearby intensity move justifies extra investigation. Moreover, new analytical strategies should be conceived and assessed to answer explicit issues that ongoing methodologies have neglected to address [4].

1.1 BACKGROUND

Scientists as of late concentrated on dependability, which is a vital essential for a fruitful and high-proficiency refrigeration framework [1-5]. The impact of the natural qualities of two-progressively work stream in the evaporator, as well as the effect of framework control attributes, can be made sense of as the wellspring of flimsiness [6]. The previous spotlights explicitly on the motions of the refrigerant's two-stage stream during the vanishing system; the result is viewed as the underlying driver of framework insecurity.

The insecurity brought about by the motions of two-stage stream bubbling, which generally applies for the most part to water frameworks like steam generators, bubbling water reactors, and reboilers, can be portrayed as static or dynamic. The static precariousness, brought about by a heating up cycle's consistent state execution, essentially incorporates Ledinegg shakiness and stream design progress flimsiness; the powerful unsteadiness, brought about by transient changes in the bubbling system, basically incorporates thickness wave motions, warm motions, and strain drop motions [7, 8].

To be sure, the results of the water framework have given the fundamental experience and strategies for refrigeration circle study. Be that as it may, a few differentiations can be made between two-work stream dangers in the refrigeration framework and those in the water framework. Water frameworks, for instance, are habitually open dissemination, and the vanishing pressure is manageable as a proper worth with a flood tank or a few compressible holders, while comparable compartments in refrigeration frameworks don't have such capabilities; the intensity transition of evaporators tubes in water frameworks is regularly a lot higher than those in refrigeration frameworks; and the functioning circumstances in a refrigeration framework, like choking, are additionally not quite the same as those in a water framework. These differentiations might represent the shortfall of certain types of motions. Besides, they are obstacles to applying the thoughts and aftereffects of water two-stage stream insecurities to refrigeration frameworks. A few past examinations zeroed in on the warm person of refrigerant with different sorts of cylinders, yet the framework design is indistinguishable from the water framework. Just [9] investigated the solidness limits of drawn out thickness wave motions in an electrically warmed single channel, up-stream framework with R-11 as the test liquid.

[1] revealed early trial perceptions of two-work stream hazards in a refrigeration framework. [2] found an oscillatory movement of the combination fume progress point in an evaporator, and the movement was accepted to be oscillatory significantly under consistent stream conditions. A few researchers, including [1], [5], and [10], suggested that the event of slug stream at the entry of the evaporator ought to have brought about the swaying; and that the slug stream ought to be a sort of warm wavering or the result of thickness wave motions. In the interim, [2] thought it was associated with the thickness wave swaying. Moreover, [11] guaranteed that it very well may be impacted by the intensity move coefficient's huge

nonlinearity. Notwithstanding, heat move coefficient variance could be an incorporated consequence of thickness wave swaying and different motions, for example, pressure drop wavering. As a general rule, in light of the fact that only a couple of trial studies have zeroed in on vanishings in refrigeration frameworks, there is not a great reason or exploratory affirmation for refrigeration framework dangers.

1.2 MOTIVATION AND PROBLEM STATEMENT

The importance of accurately predicting flow boiling heat transfer coefficients has been well recognized, as a large number of analytical and experimental investigations have been conducted by many researchers. A knowledge of these coefficients and their parametric behavior can help improve the accuracies of models used for designing and optimizing heat transfer equipment, such as evaporator and condenser. The main focus in this study is to compare boiling two-phase flow heat transfer coefficient of pure ethanol for the available experimental datasets with the theoretical datasets generated by different flow boiling correlations.

1.3 CONTRIBUTION

Multiphase flow, the simultaneous flow of different phases (states of matter) gas, liquid, and solid, is greatly influenced by gravitational level and direction, as these determine the spatial distribution of the phases with varying densities. Numerous contemporary examinations focus on the way of behaving of fluid strong streams (like in blending, gem development, or materials handling) or gas-strong streams. (for example in twisters or ignition gear). The more perplexing fluid fume or fluid gas motions found in airplane warm control frameworks, life sciences frameworks, and charge frameworks, then again, are of extraordinary interest. The peculiarity of fluid fume stream in aeronautical two-stage warm control frameworks turns out to be very perplexing because of intensity and mass trade between the two stages by means of dissipation or buildup. In spite of the fact that there are numerous distributions on two-stage stream and intensity move (course readings, gathering procedures, and diary articles), there are not many on the impact of lower gravity. This is the significant justification for completing microgravity research. This part looks at various intensity and mass exchange research concerns connected with two-stage heat transport innovations for space applications. It focuses on the most difficult instance of intensity and mass trade in

fluid fume stream. Easier cases, for example, adiabatic or isothermal fluid fume stream or fluid gas stream, can be gotten straightforwardly from the fluid fume case by focusing out key factors in the constitutive conditions. The discussions start with an outline of the exploration, trailed by a wide outline of two-stage stream and intensity move processes. The gravity level's impact will be surveyed. The subject then moves to hypothetical work on the side of improvement, tending to different components of gravity level ward two-stage stream design planning and buildup, as well as warm/gravitational scaling of two-stage stream and intensity move in various areas of two-stage warm control circles. The finishes of the hypothetical exercises are contrasted with the discoveries of many tests done on the planet (one-g) and in microgravity conditions.

1.4 THESIS ORGANIZATION

The thesis describes the model used to detect the small objects from a video sequence using the concept of deep learning. The entire thesis is divided into six chapters. The work focuses to improve the accuracy and the execution time of detecting the objects of different sizes from a video sequence.

Chapter 2 This chapter presents the survey on various approaches. However, literature survey specifically related to different applications and models specific to that of object detection is discussed, whenever the corresponding chapter is elaborated.

Chapter 4 This chapter focuses on the implementation of the proposed work carried out in object detection and recognition and the results are compared with the proposed approach.

Chapter 5 (Conclusion and Future Work): In this chapter, the conclusions are drawn from various implementations mentioned above as discussed. Future research directions are also mentioned in the chapter.

2. BACKGROUND

The most vital phase in accomplishing the task's targets is to gather information and data on the air conditioner framework utilized in the past age of the Fiat 500e, whose occupation is to execute cooling exercises (the warming tasks were satisfied by a PTC radiator). The strategy of social event information and fostering the vehicle's refrigerant circle model utilizing the one-layered programming Amesim is examined in this section. To achieve thus, the cycle executed, and the framework parts required are first depicted. The demonstrating approach used to come by the end-product is then characterized [12] [13]. This procedure can be detached into two full scale fragments, which can then be segregated into two extraordinary parts, for an amount of four following stages. Figure 2.1 shows these periods. The primary partition is between individual part demonstrating and the structure of an entire framework level model. The principal stage is to find the ideal match between the virtual and genuine parts planned in Amisom. To arrive at this objective, the client should go through two phases: a primer mathematical definition, trailed by a thermodynamic execution adjustment. When every part has accomplished the most ideal (and sensible) coordinate with its genuine partner, they can be converged to make a full framework level model [14][15]. This activity's essential outcome is to characterize the ideal worth of the virtual coolant charge, which will be completely determined later in the part. At last, the model overall will be approved by contrasting its reproduction discoveries with genuine seat test information. This will exhibit the model's accuracy and reliability, permitting specialists to involve it later on. The libraries open in the underlying system contain data about the properties and numerical model of the Amesim parts [16].

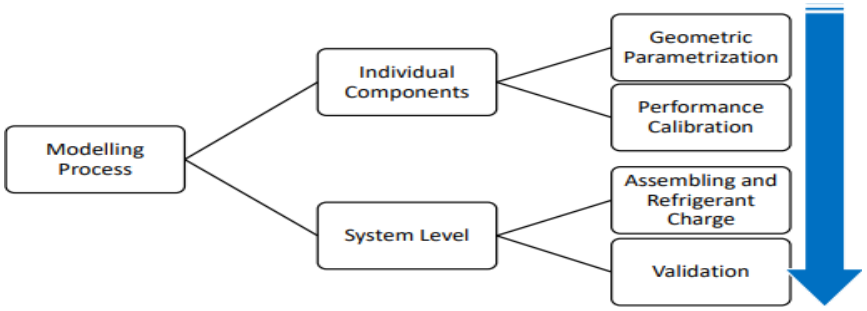

Figure 2.1: Phases of The Modelling Process Followed to Build the AC System for the Refrigeration Loop.

2.1 DESCRIPTION OF THE LOOP

The fluid in the evaporators will assimilate the intensity load. Thus, the fluid will to some degree dissipate. The two-stage stream from the evaporators is presently shipped off the condenser (see additionally figure 2.2), where it consolidates to liquid. The liquid may now be diverted to the evaporators [17][18]. To move toward inundation, a preheater is utilized to help the temperature of the liquid before it enters the evaporators. In the two-stage stream, a detour is made so the great impact of this preheater might be shown during tests. The strain and temperature in the framework are constrained by the collectors [19].

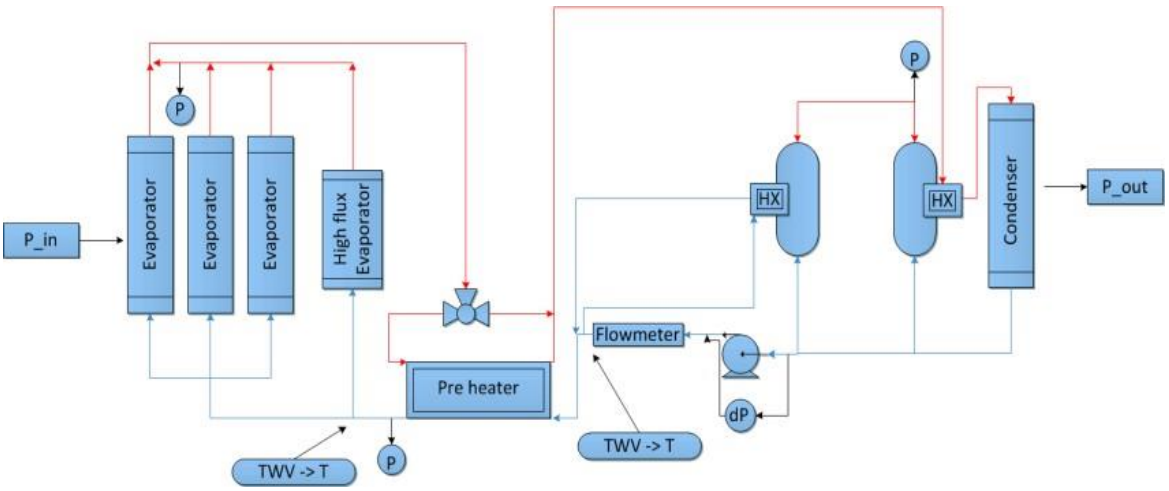

Figure 2.2: Schematic Overview of The Two-Phase Loop.

A 3D model was created, and the setting was built. The main difficulty was an enormous hole (or various breaks) in the siphon (likewise missing in the image).

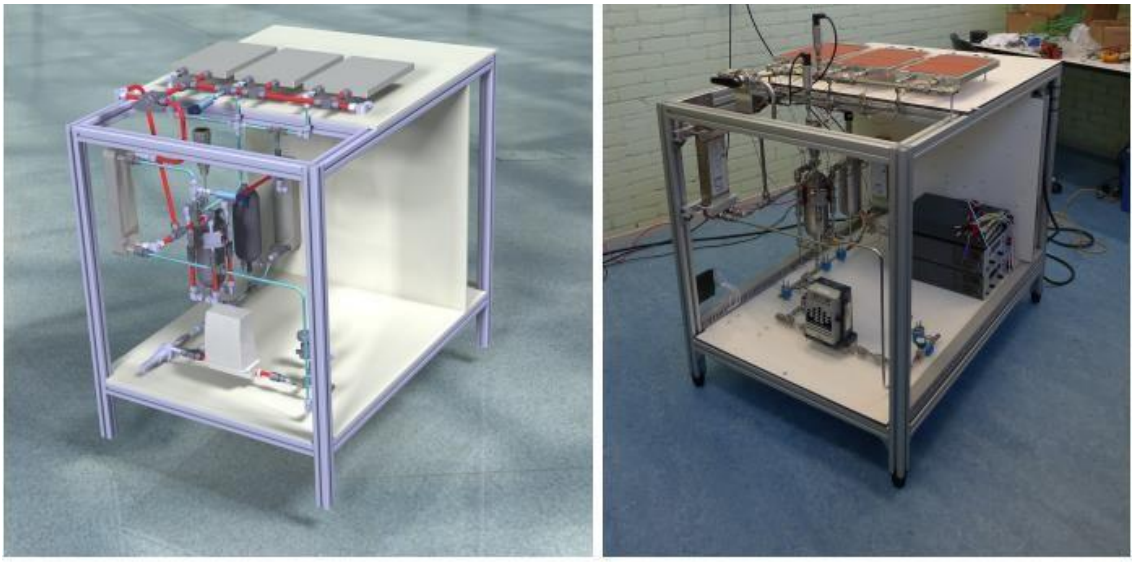

(a) Model (b) Setup

Figure 2.3: Setup Design and Actual Setup

2.2 VAPOUR-COMPRESSION CYCLE – COOLING LOOP

The reason for a warming, ventilation, and cooling (air conditioning) framework can be characterized as three particular principal capabilities: temperature control, which is achieved by adding or eliminating heat from the vehicle lodge; dampness control, which is achieved by dehumidifying or drying the endlessly air flow control, which is achieved by recycling and supplanting lifeless air [19]. The Air conditioner framework viable is responsible for cooling the vehicle lodge in sweltering weather patterns, and it works by utilizing a liquid known as refrigerant (for this situation R134a). Two graphs portray a praiseworthy cycle: the temperature-entropy chart and the strain enthalpy outline [20]. This framework is comprised of four fundamental parts (blower, condenser, thermostatic development valve, and evaporator), every one of which plays out an alternate thermodynamic change of the functioning liquid. The thermodynamic changes are as per the following: pressure (heat move at consistent tension from the refrigerant to the outer air); development (heat move at steady strain from the refrigerant to the inner air); and a subsequent intensity move at steady tension with the air streaming inside the lodge towards the refrigerant. Since the refrigerant goes through a stage progress during both isobar processes, three unmistakable advances can be recognized. To start, the refrigerant gas is cooled to the place of submersion in the condenser, where adequate power is dispensed with

as the temperature diminishes during the cycle [21]. Second, the gas is thick in liquid refrigerant, causing the drenching direct temperature toward stay steady as the torpid force moves. At long last, the liquid refrigerant could go through a further cool down, otherwise called subcooling, to ensure that all of the refrigerant has consolidated. Also, the fluid refrigerant in the evaporator is at first warmed until immersion, when the temperature stays consistent while the refrigerant vanishes. After this activity is finished, the temperature of the refrigerant gas is brought further up in a cycle known as superheating (Figs. 2.4 and 2.5) [22].

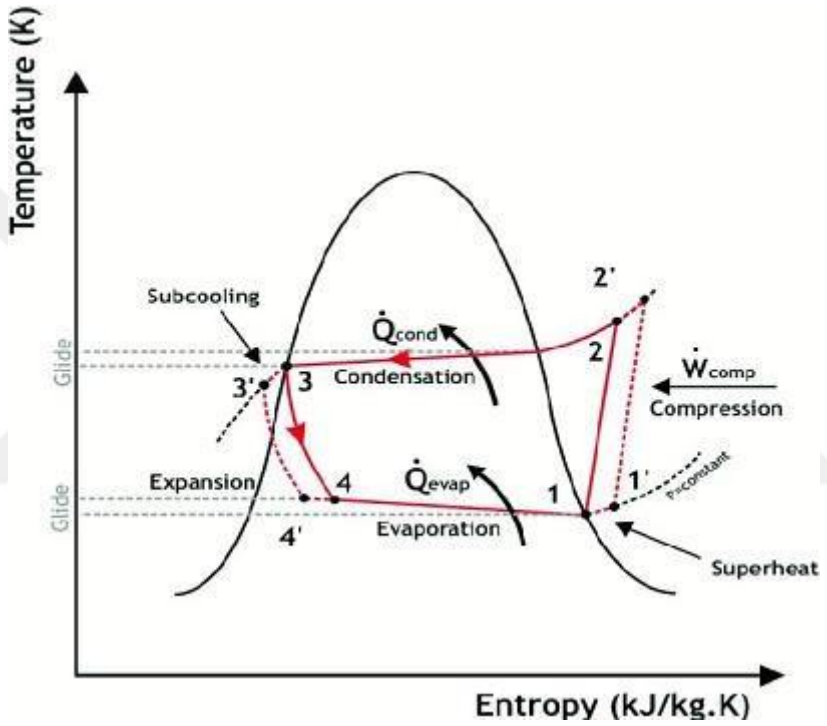

Figure 2.4: T-s Diagram of A General Vapour-Compression Refrigeration Cycle [67].

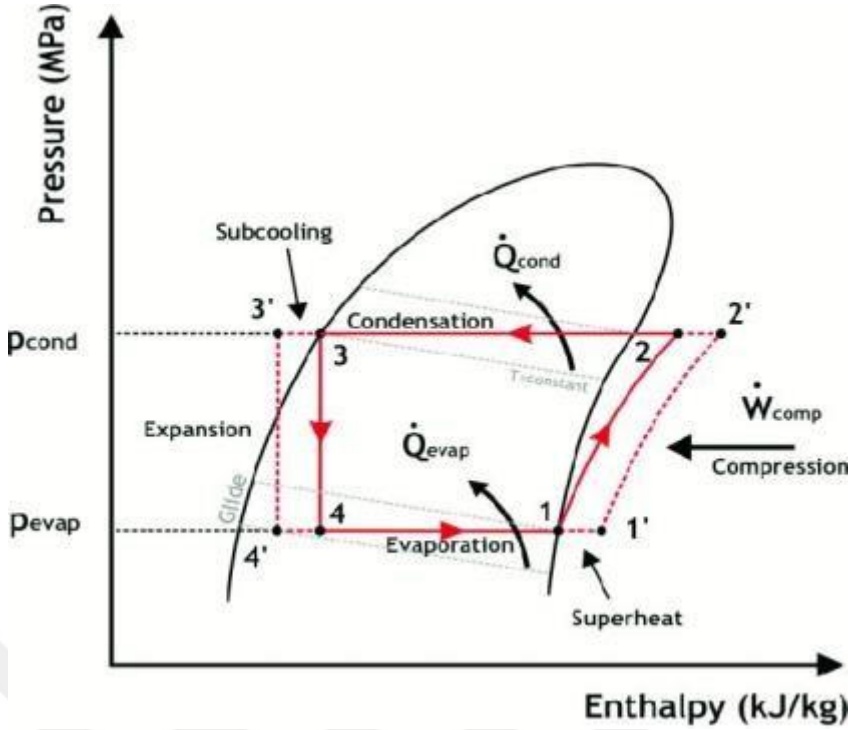

Figure 2.5: p-h Diagram of A General Vapour-Compression Refrigeration Cycle [67].

2.3 STEADY STATE MODELING

The cooling of the aggregator is viewed as far as strain drops and intensity move. For the two-stage frictional strain decline, two unmistakable relationships are utilized (Muller-Steinhagen and Hell, Friedel) [24]. Minor, gravitational, and energy pressure misfortunes are additionally thought of. Limitation tubes are intended to permit a particular intensity burden to be applied to two rather than three evaporators without totally vanishing the fluid. Over the entire circle, the absolute tension misfortune (figure 2.6) is around 0.7 bar. Around 45% of this tension drop is brought about by the limitation tube and evaporator, while the excess 18% is brought about by the gatherer's intensity exchangers and matching elbows [25]. The distinction between the two relationships used on the general tension drop of the total circle is 5%. Frictional strain drop represents the greater part of the aggregate, with moderate tension misfortune representing 40%. This is not out of the ordinary given the quantity of elbows in the framework [26].

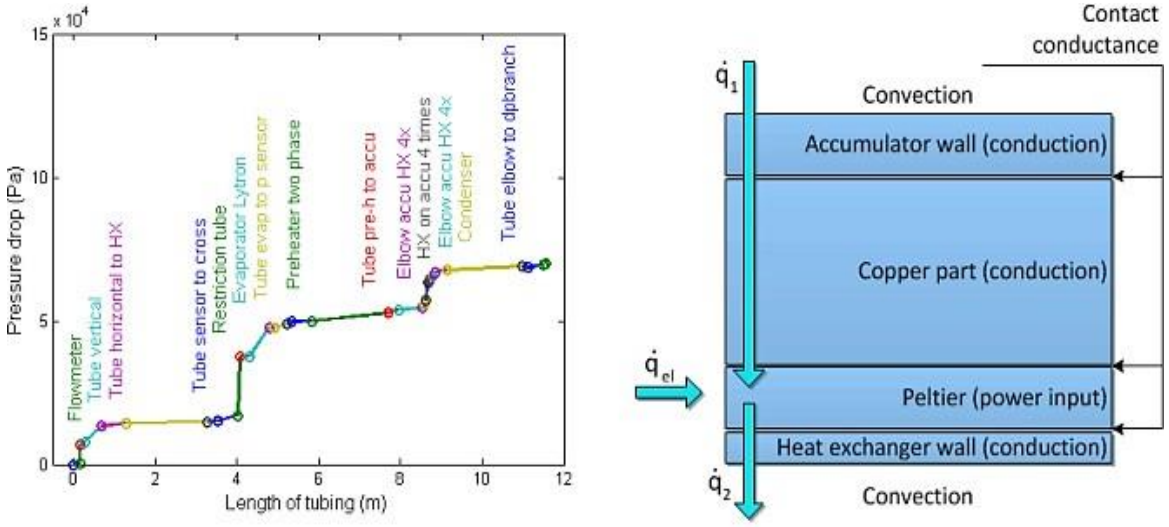

(a) Steady state pressure drop along the loop (b) 1D representation of the cooling system

Figure 2.6: An 1D Approximation of the Heat Transfer in the Cooling of the Accumulator is Modeled (figure 3b) [26].

Warm protections cause temperature changes all through the circle (figure4a). Since the temperatures in the two liquids are the same, thermoelectric modules will be utilized. At the point when power is given to these modules, a temperature contrast between the different sides is made. Four unmistakable connections are utilized for the convection of the two-deliberately ease stream in the cooling channels [27]. The contact conductance had all the earmarks of being a huge vulnerability in the model, and the various connections uncovered critical errors (figure 2.7b).

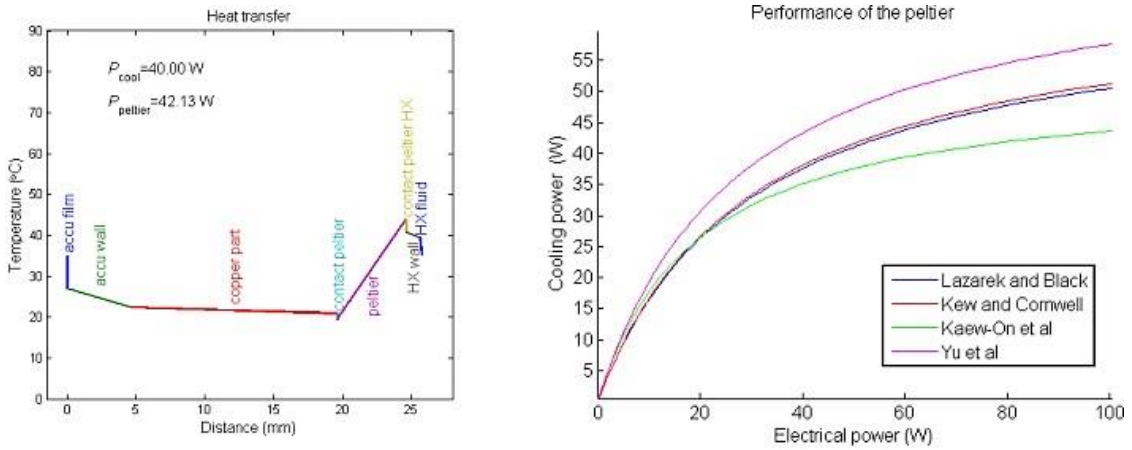

(a) Temperatures in cooling system (Kew and Cornwell) (b) Performance of different correlations

Figure 2.7: Heat Transfer in the Cooling System [29].

2.3.1 Time Dependent Model

For this undertaking, the NLR's time-subordinate model was adjusted. A couple of changes have been made, and pressure drop models have been presented. Most of the outcomes were true to form, except for the complete strain decline, which was far lower than determined (0.53 bar). The arrangement was fabricated utilizing a 3D model, which was very effective. Early upgrades were made, and the establishment went without a hitch. Estimations for consistent state conditions are performed, and not entirely set in stone [30][31]. The general tension drop is supposed to be generally 0.7 bar. Minor tension misfortune has a critical effect and ought not be ignored. There are various vulnerabilities in the intensity move gauge. The time-subordinate model has been improved and custom fitted to our task. The strain drop computation delivered a far lower result than the consistent state estimation. This is in all probability because of the utilization of an alternate stream model [32].

2.3.2 Components Modelling

The demonstrating approach, as made sense of in the presentation, starts with the mathematical parametrization of every part. When this initial step is achieved, the aspects and other mathematical properties of the virtual parts will be indistinguishable from the genuine ones. Since there is no exact and unambiguous relationship among calculation and thermodynamic way of behaving, this mathematical consistency among reenacted and genuine component is lacking to lay out a practically equivalent to connection in their presentation [33]. Subsequently, it is basic to align the conditions responsible for thermodynamic computation utilizing exploratory information. Every part's parametrization and adjustment method is extraordinary and rigorously attached to its elements. The methodologies used for every part are portrayed in the passages that follow [34].

2.4 HEAT TRANSFER CALCULATIONS (1D)

At the point when the intensity load changes, so does how much fluid vanished per time unit. This implies that the fume mass part and, thus, the thickness will change. Fluid will currently stream into and out of the gatherer, prompting strain and temperature in the aggregator and all through the framework to change [35]. At the point when a uniform framework temperature is wanted, a two-stage mechanical siphoned circle is ordinarily utilized. To get

back to the ideal temperature, a collector is used to control the strain in the know. There are two sorts of aggregators: heat controlled gatherers and tension controlled collectors (see figure 2.8) [36]. Warmers can dissipate a portion of the fluid on the lower part of the gatherer to support pressure, and as tension drops, the highest point of the collector is cooled [37].

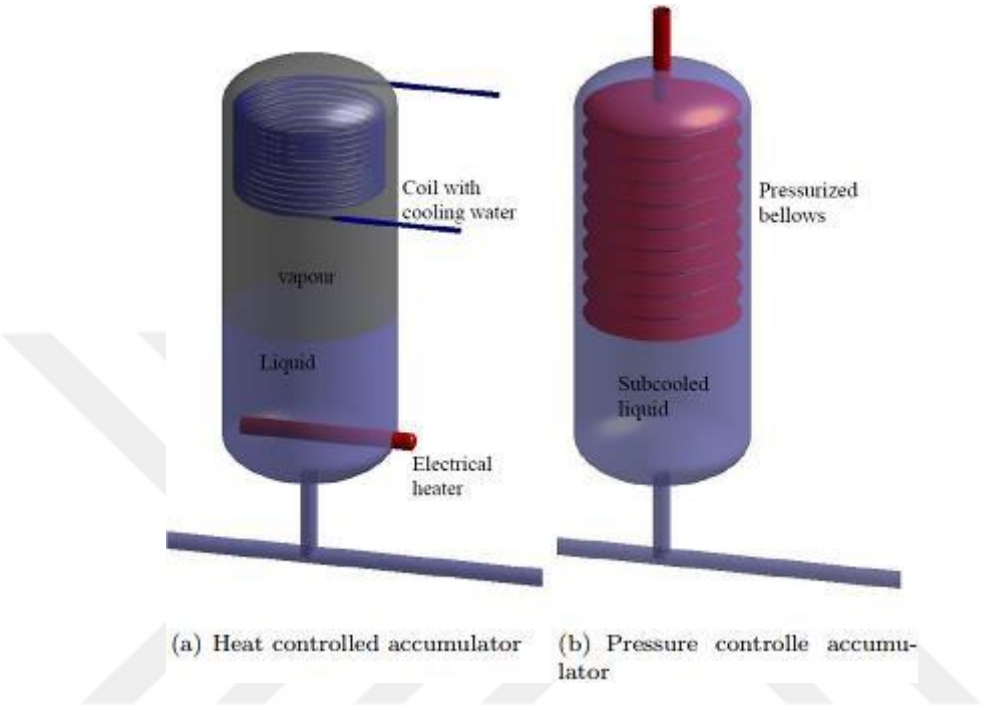

Figure 2.8: Two Types of Accumulators [37]

The intensity move in the evaporator's warming foil is displayed in the last part. To abstain from overheating, the greatest intensity burden ought not set in stone.

2.4.1 Heating Capacity Accumulator

Warming can be achieved by various strategies, including welding heat exchangers to the cell wall or utilizing electrical radiators. Warming in this circle is given exclusively by two electrical radiators situated at the base piece of the aggregators, as displayed in figure 4.9 [38]. All power will be conveyed into the liquid as long as the warmers don't overheat. At the point when the radiators are turned on, it is resolved how much the cooling system needs to cool before the warming is diminished [39][40].

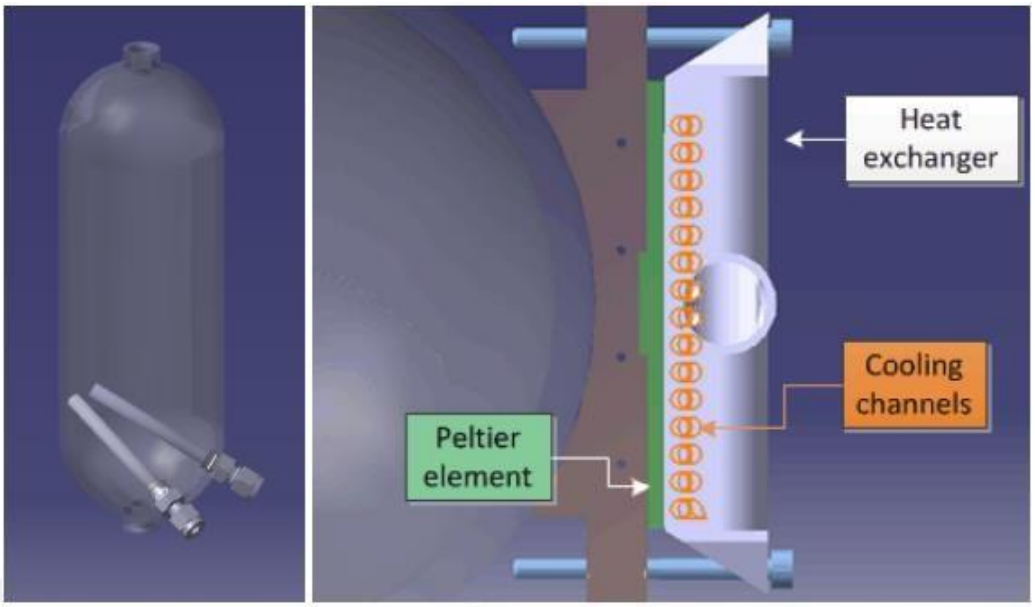

(a) Heating components in the accumulator (b) Top view of the cooling system on the accumulator

Figure 2.9: Cooling and Heating in the Accumulators.

2.4.2 Cooling Capacity Accumulator

There are additionally a few strategies for cooling the fumes in the gatherer's upper segment. To put it plainly, they are ordered into two kinds: frameworks that straightforwardly cool the fluid and frameworks that cool the aggregator wall [41]. Heat exchangers were decided to cool the aggregator's wall. As a cooling liquid, sub-cooled fluid stream or two-stage stream can be utilized. Since the fluid should stay fluid and subsequently can't be warmed definitely, two-stage stream is utilized [42][43]. This stream can take a ton of intensity without warming up, yet it has a similar temperature as the two-progressively work stream in the collector, hence a temperature differential ought to be created. This is achieved by the utilization of thermoelectric modules. Electrical energy will be utilized in thermoelectric modules to pass heat from one side on to the next (the Peltier impact). Thus, one side will turn into a cooling plate [44].

There are a couple of warm protections between the cooling plate and the liquid in the collector. Since the cooling limit is profoundly reliant upon the upsides of these warm protections, estimations on heat move from the two-progressively ease liquid in the gatherer to the two-deliberately work stream in the intensity exchanger are performed [45].

2.5 OVERVIEW OF TWO-PHASE FLOW REGIMES

In the high heat flux cooling solutions of interest, the phases constituting the two-phase flows are liquid and vapor. As vapor is generated by absorbing heat, the volume of vapor in the liquid flow continuously increases and causes the flow to evolve sequentially through flow regimes that can be identified by visual appearance [46][47][48]. Each flow regime performs differently in terms of heat transfer and pressure drop, and therefore understanding the flow regime evolution aids in understanding the fundamental fluid physics leading to that performance [49][50].

In macroscale flows, the four main flow regimes were identified and described by [51][53]. These regimes were stratified, dispersed bubble (bubble), intermittent (slug), and annular. These flow regimes are shown in Figure 2.10. One of the identifying factors of macroscale flows is that gravity has a significant influence on the morphology of the flow, causing horizontal flow to be asymmetric about the pipe axis at low quality, with the heavier liquid tending to flow along the bottom and the lighter vapor along the top [54]. For simplicity, stratified flow and wavy stratified flow will be identified here simply as stratified flow. In the dispersed bubble regime, the vapor phase consists of small bubbles mixed with the liquid phase; in this regime, the bubbles are driven axially at approximately the same speed as the liquid. The buoyancy of the bubbles may lead to a higher concentration of bubbles at the top of the tube [55].

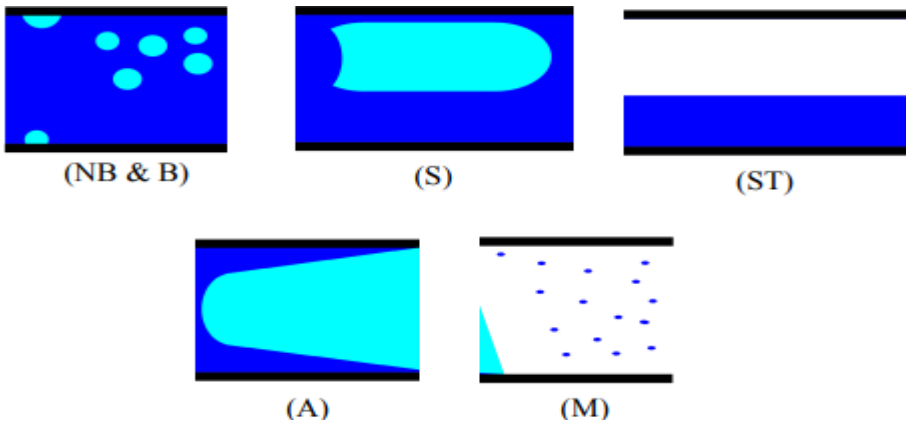

Figure 2.10: Illustration of Flow Regimes in Macroscale Channels. Nucleate Boiling and Bubble Flow (NB & B) at Low Quality, Slug Flow at Intermediate Quality (S), Stratified Flow May Alternatively Occur at Intermediate Quality (ST), Annular Flow at Higher Quality (A), and Finally, Mist Flow (M).

As quality increases, the intermittent (slug) regime occurs. In this regime, the smaller bubbles have coalesced into larger “slugs,” that have cross-sectional area comparable to the pipe cross section but separated by liquid “plugs.” In the stratified regime, the liquid and vapor phases are separated into layers, in which the buoyant gas phase flows along the upper part of the cross section while the heavier liquid phase travels along the lower part [56][57]. As the void fraction of the vapor increases, the high velocity vapor flow tends to drive the liquid phase into an annular ring lining the entire perimeter of the tube cross section with the vapor core flowing through the center. As more liquid is converted to vapor, the annular liquid film becomes depleted, leading to film rupture and local dry out [58].

Film depletion continues until the flow is single-phase vapor. Several flow phenomena may cause liquid droplets to become entrained with the vapor flow as the vapor flow interacts with the bulk liquid, including bubbles erupting through the liquid-vapor interface, turbulent fluctuations in the vapor, and vapor shear on the nonuniform liquid film. The entrained liquid is often broken into droplets by the turbulent vapor phase, generating the “mist” flow regime [59].

Flow regime evolution occurs in microscale flows in a similar fashion in macroscale flows, but the forces imposed by gravity become less dominant while surface tension and viscous shear become much more influential, as can be shown though dimensionless groupings found in Appendix 9.1. The increasing role of surface tension relative to gravity is evidenced by the shrinking Bond number with decreasing hydraulic diameter. The increasing influence of surface tension over inertia is evidenced by the shrinking Weber number with decreasing hydraulic diameter, and similarly, the increasing influence of viscous shear over inertia is evidenced by the decreasing Reynold’s number with decreasing hydraulic diameter [60]. The general flow phenomena occurring in microscale flows are illustrated in Figure 2.11.

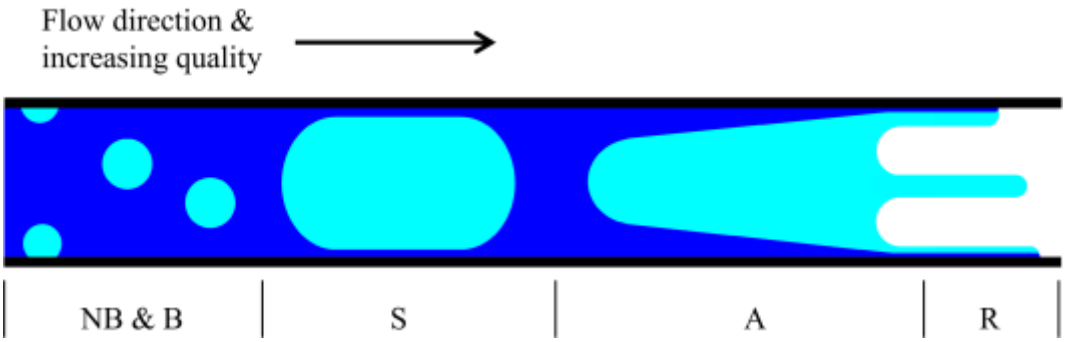

Figure 2.11: Illustration of Flow Regimes in Microscale Channels.

Nucleate boiling and bubble flow (NB & B) at low quality, slug flow at intermediate quality (S), annular flow at higher quality (A), and finally, rivulet flow (R).

The increased influence of surface tension and shear causes microscale flows to become more axisymmetric; the stratified flow regime is typically not reported in microscale flows [61]. The symmetry of microscale flows is also manifested in the more uniform film thickness around vapor slugs flowing in horizontal channels. The circumferential film thickness variation is measurable, and the uniformity has been used as an empirical criterion to predict the transition from micro to macroscale flow behavior. The Confinement number indicating the transition is shown in Equation (5), and it can be observed that this dimensionless group is simply the inverse square root of the more commonly used Bond number [62].

$$C_O = \frac{1}{D_h}\sqrt{\frac{\sigma}{g(\rho_L - \rho v)}} \tag{2.1}$$

In Equation (5), Dh is the hydraulic diameter, $\rho\rho$ is the liquid (subscript – L) and vapor (subscript – V) density, $\sigma\sigma$ is surface tension, and g is the acceleration due to gravity. In the study, a Confinement number of 0.5-1 indicated that the transition from macroscale to microscale. In the current study, Co = 4.6 for FC-72 and Co = 6.2 for R245fa, both well within the region considered to be dominated by microscale phenomena. In another study, viscous shear was incorporated into the empirical criteria predicting a transition in flow behavior from microscale to macroscale with Reynolds number–Bond number product, referred to as a "convective Confinement number" [43]. This convective Confinement number incorporates effects from both viscous shear and flow velocity, and therefore, may be a more universal indicator for the flow conditions under which microscale or macroscale

flow phenomena occur. Within the annular regime, uniformity of the liquid film thickness around the perimeter of the channel is also increased in microscale flows compared to macroscale, because of the increased influence of surface tension and viscous shear.

Furthermore, because of the increased influence of viscous shear, as well as the small channel diameter, the vapor flow in the microscale annular regime is much less likely to be turbulent. Lack of turbulence combined with various wettability effects can give rise to "rivulet" flow in the high quality annular regime. This condition occurs when liquid ribbons form on the channel wall in the streamwise flow direction, driven in a meandering path by vapor shear [56].

Phenomena that can cause liquid to become entrained with the vapor can still occur in microscale two-phase flows. These phenomena include non-uniform liquid film thickness (waves, rivulets) and low liquid wettability (high contact angle) to the solid surface [56]. The absence of turbulence also decreases the breakup of liquid films into smaller droplets, and facilitates an increased probability of "filament" flow. Filament flow occurs when thread-like liquid formations flow along the center of the channel with little contact with the walls.

2.6 OVERVIEW OF TWO-PHASE FLOW HEAT TRANSFER

As recently expressed, the two-stage stream systems are inseparably connected with heat transmission from the channel wall into the liquid. This segment will generally focus on microscale two-stage streams. As per Forster and Zuber [51], bubbles start to frame at nucleation destinations, which are regularly looking like a little crevice, with adequate wall superheat (wall temperature increase over the nearby liquid immersion temperature). The air pocket grows when fluid in it is gone to fume. This is the essence of nucleate boiling. With forced convection, the stationary bubbles on the channel wall disrupt the liquid boundary layer, and may enhance single phase convection into the liquid. With sufficient size, the drag caused by the hydrodynamic boundary layer causes the bubbles to become entrained in the liquid flow. Increasing volume of bubbles in the flow causes the flow to accelerate, thinning and possibly further disrupting the thermal boundary layer. A large concentration of bubbles in the liquid flow causes the bubbles to agglomerate into larger bubbles, and eventually slugs.

In slug flow, the single-phase heat transfer continues to occur within the liquid plugs between slugs. The dominant mechanism of thermal transport from liquid to vapor may be in one of two forms: convective boiling or nucleate boiling. In diabatic microchannel visualization studies, both have been observed in annular liquid films [63]. Convective boiling (thin film evaporation) occurs via heat conduction from the wall through the liquid film into the convecting vapor core, in the absence of bubbles nucleating on the channel wall. Contrarily, strong evidence of nucleate boiling has also been reported in annular films [64], though the likelihood of nucleate boiling decreases as the wall superheat falls. The channel cross-sectional shape, surface roughness, and other variables often differed between contradictory studies, and may be important factors in determining the primary heat transfer modality. Regardless of the heat transfer mechanism, fluid-solid properties including wettability, surface roughness, surface tension, slug velocity, liquid viscosity (Capillary number), heat flux, and other factors, may allow the liquid film surrounding vapor slugs to locally dryout, causing locally low HTC's [65].

At a sufficiently high vapor quality, the flow transitions into annular flow, in which the thermal transport may either be dominated by convective boiling, or, perhaps, small-scale nucleate boiling. Regardless, the liquid film eventually becomes too thin, and susceptible to local rupture and dryout [66]. Dryout and rewetting is often cyclical, and results in large temperature fluctuations (40°C) in this region [67]. In the transition from annular flow to dryout, rivulet flow can occur. In addition to the adiabatic phenomena that cause rivulet flow, the temperature dependency of surface tension (Marangoni effects) and temperature-dependent wettability effects may also play a role. In this post-dryout regime, local and intermittent dryout occur. The liquid ribbons flowing along the wall continue to evaporate, while a significant portion of the wall may be exposed to vapor, causing HTC's to decline in this flow regime [68].

Filament flow may also occur in diabatic microscale two-phase flows. In addition to the causes of liquid entrainment in the vapor described in the previous section, Marangoni effects and temperature-dependent wettability effects may also play a role. The filament regime is post-dryout, because the vapor is consistently in contact with the walls. Evaporation of the liquid entrained with the vapor only occurs when the vapor is sufficiently superheated [69]. This post-annular flow produces HTC's much lower than the HTC's

produced at qualities leading up to dryout. Filament flows expose large wall areas directly to the heated vapor, causing widespread—but not total dryout—and can enable dryout to occur at much lower mass fractions of vapor (quality) than 100% [70][71]. At 100% quality, the flow becomes single-phase vapor, which produces relatively low HTC's, but continues to absorb heat through convective, sensible heating. The following sections discuss useful literature that quantifies the most relevant phenomena discussed up to this point [72].

2.7 SUMMARY OF TWO-PHASE FLOW RESEARCH MOTIVATION

A solitary channel inside a complex microchannel cooler is a particular math that shifts from other frequently investigated two-stage stream calculations. Microscale pressure driven breadth, high angle proportion cross segment, little length comparative with water powered width (L/Dh 100), and U-molded stream section by means of the channel are key differentiations. Every one of these differentiations, and their joined effects, has suggestions for stream peculiarities and intensity move that are not broadly revealed in the writing. This study seeks to research and characterize these effects in the pursuit of greater understanding of the parametric effects, greater predictability, and further performance enhancement in high-heat flux, embedded electronics coolers.

In recent years, there has been a surge in interest in the use of heat pipe technology for heat recovery and energy savings in a wide range of technical applications. Heat pipes are turning out to be more fundamental in numerous modern applications, especially in upgrading energy reserve funds in business applications and further developing intensity exchanger warm execution. In view of their comprehensiveness, adaptability, accuracy, and productivity, computational methodologies assume a fundamental part in taking care of muddled stream issues for an extensive variety of designing applications. Notwithstanding, in light of the fact that to the intricacy of multiphase stream qualities and intensity and mass exchange stage advances, computational examinations on heat pipes are still in their beginning phases. Subsequently, the essential objective of this exploration is to make a CFD model that consolidates the confounded actual peculiarities of both the intensity move cycles of vanishing and buildup, as well as the mass exchange interaction of stage change during pool bubbling and film buildup.

3. PROPOSED SYSTEM

3.1 MOTIVATION

The consistent interest for development in heat move answers for more reduced and strong hardware is driving examination toward new advancements fit for dispersing more power in less space while keeping up with high dependability norms [1]. Heat management research has been pushed toward the improvement of another age of procedures in view of two-stage advancements to meet rigid necessities of conservativeness and high intensity motions, to accomplish compelling, solid, and modest intensity move in brutal conditions like space. These advantages are acknowledged through a significant degree expansion in heat move coefficient accomplished with stream bubbling and buildup over single stage frameworks [2].

The most ideal way to present the idea of latent two-stage heat move gadgets, and afterward Throbbing Intensity Lines as individuals from this family, is to give a general point of view on the essential ideas fundamental the different intensity move advances accessible [12][13]. This will lay out situation among the different heat management arrangements accessible. On the off chance that a heated item should be cooled to abstain from overheating and to keep a plan temperature, different cooling strategies can be utilized (Figure 1). Six classes are proposed by a conventional general order [14]:

- Radiation - Natural gas cooling - Natural liquid cooling - Forced gas cooling - Forced liquid cooling - Cooling in two phases Expecting that the outside heat move coefficient is known and fixed (as in convective air cooling), the easiest procedure to further develop cooling productivity is to expand the trade surface with a progression of strong balances [15] [16]. For this situation, the warm conductivity of the material, along with the extension of the exchange surface, will characterize the limit in heat move. One more methodology for successfully cooling the item is to course a liquid in a shut circle that interfaces the intensity source (object) and an intensity sink, using reasonable intensity move (single stage siphoned circle) or permitting the liquid to disintegrate to use both reasonable and idle intensity (two stage siphoned circle); expanding the Reynolds number compelling the flow with a siphon will build the intensity move [5]. Constrained convection isn't restricted by framework direction; however, it raises framework costs and diminishes framework dependability and

minimization. Thermal conductivity can be extraordinarily expanded by supplanting the strong conductive blades with a detached two-stage gadget, for example, a thermosyphon, which utilizes both conductive and inactive intensity move components. Thermosyphons are gravity-helped gadgets that will experience issues because of gadget direction [6]. An Intensity Line can beat this limit by utilizing a permeable media to guarantee the arrival of condensate to the evaporator paying little heed to tendency, but at a diminished exhibition. Throbbing Intensity Lines can utilize both reasonable and dormant intensity move, disposing of the requirement for a siphon and wick to diminish intricacy and accomplish heat management that is practically free of direction [17].

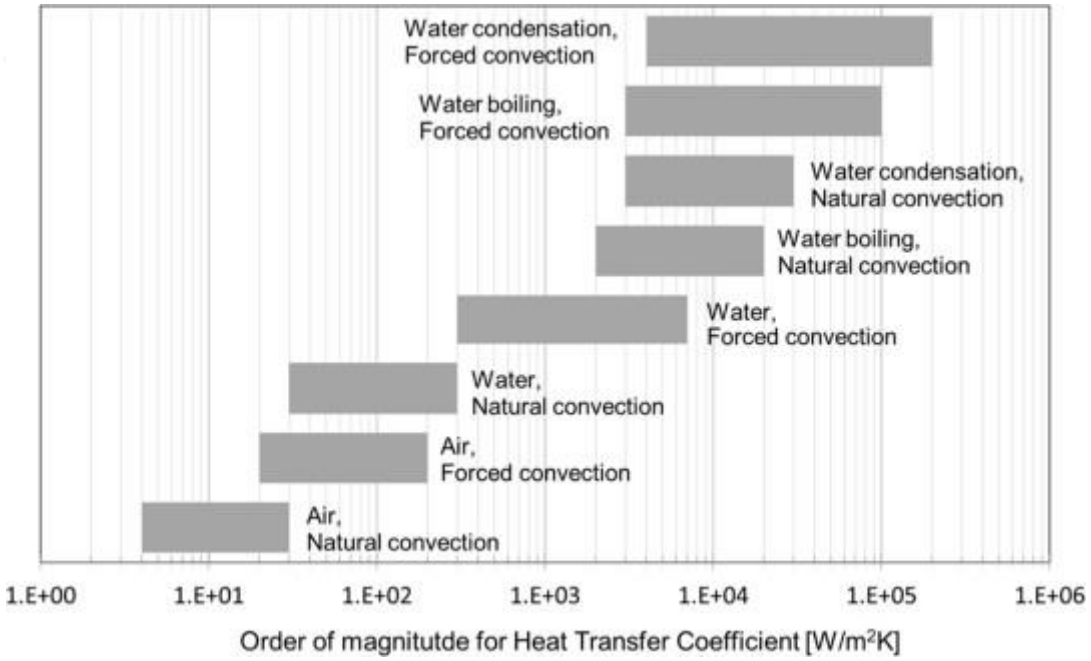

Figure 3.1: Order of Magnitude of Heat Transfer Coefficient Achievable With Different Cooling Technologies [18].

Complex devices have more and more electronic components. However, as the power surges, heat production becomes important. It is therefore necessary to evacuate it to ensure the proper operation of the appliance. This evacuation can become a vital system for the latter in some cases. This is the case in satellites, which are based on the proper functioning of their equipment. However, the evacuation of the heat is here particularly delicate because the mechanisms involved are limited [7][19].

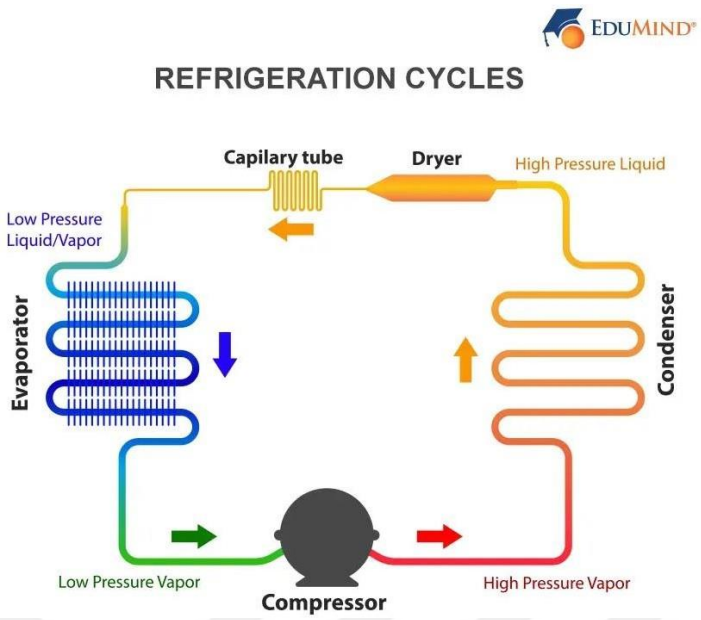

Figure 3.2: Working Cycle of Refrigeration System [7].

In fact, on board a satellite, the heat is mainly emitted by radiation at the level of the external panels. The purpose of this project is to study a cooling loop, from the condenser to the evaporator. In our case, the refrigerant fluid circulates in a test evaporator, the electronic components being replaced by imitators producing only heat. This heat is subsequently evacuated by vaporizing the fluid when passing the fluid at the component level. A diphasic flow occurs in the evaporator. This method is more efficient than a conventional cooling, in monophasic flow, because the flow of heat transported is more important [8]. This system has a considerable advantage over the capillary pumping system: the radiation temperature at the condenser level is about 100 °C vs. 40 °C with a conventional heat pump system. This makes it possible to reduce the surface of the side panels by 60% and therefore the weight of the installation. However, due to the diphasic flow, the simulation of it is more delicate [9][20].

3.2 RESEARCH OBJECTIVE

The project deals with the sizing of an evaporator for a thermal control loop of a telecommunication satellite. The objective is to develop a MATLAB code in order to calculate different parameters of the evaporator, such as the pressure losses within the evaporator, or the temperature of the components, in order to validate the load specifications: Do not have a loss of pressure too large or do not exceed a critical value for the temperature of the components. We will have to take the right simulation models according to the convective boiling regime (in diphasic), in which we find ourselves. We also need to consider the loss of load that can occur at the level of our flow, and especially the singular load losses here. In fact, the presence of the elbows will lead to load losses. The problem is that these losses are difficult to model because our flow is diphasic. To do this, we need to use experimental studies that have already been carried out. In order to characterize our convective heat exchanges in the tube, diphasic correlations will be used to calculate a heat-exchange transfer coefficient (h) that will therefore be variable within our flow.

3.3 TWO-PHASE FLOW AND HEAT TRANSFER

The simplest form of multiphase flow is two-phase flow, which is the simultaneous flow of different phases (states of matter): gas, liquid, and solid. In spaceship thermal control systems, two-phase flow has a single component, which means that the vapour and liquid phases are the same chemical material. When the phases are made up of separate chemical substances, as in air-water flow, the flow is referred to as two-phase two-component flow. The same mathematical model equations describe flow-related (hydraulic) two-phase, single-component, and two-component flows. Subsequently, aftereffects of computations and tests in a single framework can be utilized in the other for however long they are restricted to stream peculiarities and don't include heat move. Heat move essentially affects framework conduct in a two-stage two-part framework: just the physical (material) characteristics of the stages are temperature dependent. Two-stage single-part frameworks are essentially more muddled on the grounds that heat transmission and temperature produce mass trades between the stages by means of vanishing, blazing, and buildup, notwithstanding changes in the actual properties of the stages. Thus, utilizing the displaying and trial aftereffects of less complex two-stage two-part frameworks, perplexing two-stage single-part frameworks can't be totally fathomed. Two-stage single-part frameworks, for example,

the fluid fume frameworks utilized in spaceship temperature control circles, require their own, very perplexing numerical displaying and committed two-stage single-part analyzes.

Although all basic fluid physics concepts apply to liquid-vapour flows, their constitutive equations are more numerous and complicated than single-phase flow equations. The difficulties originate from the fact that the effects of inertia, viscosity, and buoyancy may be attributed to both the liquid and vapour phases, as well as the influence of surface tension effects. The flow pattern, or geographical distribution of liquid and vapour, adds an additional and substantial issue. Through the fundamental (morphological) patterns for bubbly, slug (or plug), annular, and mist (or drop) flow, the arriving pure liquid progressively transitions to the outgoing pure vapour flow. The bubbly-slug, slug-annular (churn), and annular-wavy-mist hybrid flow patterns can be thought of as transitions between primary patterns.

The issue is that each flow pattern (regime) necessitates its unique mathematical model. Transitions from one pattern to another must also be simulated. Within a regime, additional criteria can be used to refine the modeling: the magnitudes of various forces or the distinction between laminar and turbulent flow,

3.4 PROPOSED SYSTEM

In order to best model the thermo-hydraulic phenomena, we have used different diphasic models. Due to the results of the preliminary studies, the inlet flow of the evaporator is assumed to be annular with the gas circulating in the middle of the pipe and the liquid lying at the level of the wall. The heat emitted by the electronic components will cause the liquid to change phase. The steam title will grow, and the surface speed of the gas will increase. Due to the difference in speed between gas and liquid, there is going to be a tearing of liquid droplets at the interface between the two phases from a critical velocity. From a study carried out previously, we could see that the grubbing-up had no effect on the flow. This is surely because the number of droplets pulling out is low vis-à-vis the annular flow. Thus, we decided not to model this phenomenon of grubbing because of its negligible weight. From a purely thermal point of view, we place ourselves in a saturated boiling regime and model the heat exchange coefficient. When the title of the vapor phase is important enough to consider that the flow is monophasic, we use the monophasic thermal model. We will also note that

a singular load loss model at the elbows (valid in no gravity) has been implemented. From our various studies, we have found that the homogeneous model should be used for weaker titles, than the ones we are studying. Indeed, we find that the velocity changes are increasingly weak when the steam title is also. Finally, when the steam title is unitary, we use a monophasic model.

3.5 WORKING CYCLE

The project deals with the sizing of an evaporator for a thermal control loop of a telecommunication satellite. The objective is to develop a MATLAB code in order to calculate different parameters of the evaporator, such as the pressure losses within the evaporator, or the temperature of the components, in order to validate the load specifications: Do not have a loss of pressure too large or do not exceed a critical value for the temperature of the components. We will have to take the right simulation models according to the convective boiling regime (in diphasic), in which we find ourselves. We also need to consider the loss of load that can occur at the level of our flow, and especially the singular load losses here. In fact, the presence of the elbows will lead to load losses. The problem is that these losses are difficult to model because our flow is diphasic. To do this, we need to use experimental studies that have already been carried out. In order to characterize our convective heat exchanges in the tube, diphasic correlations will be used to calculate a heat-exchange transfer coefficient (h) that will therefore be variable within our flow.

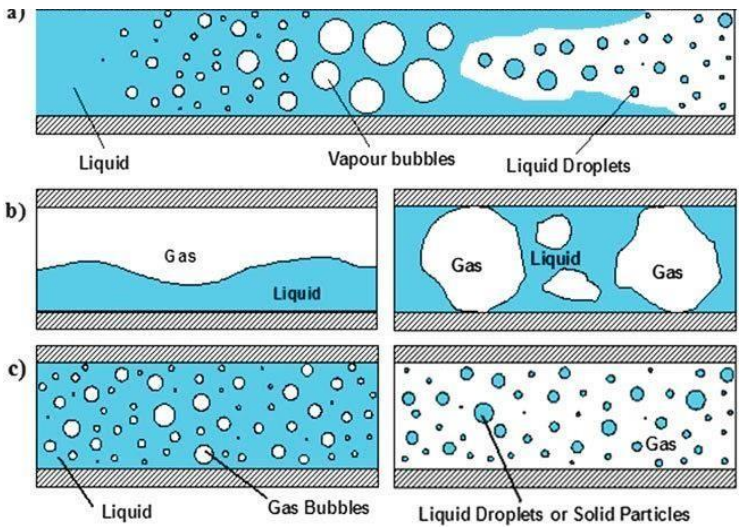

Figure 3.3: Evolution Form A Monophasic Flow to A Diphasic Flow.

The geometry is basically composed of several loops like this and can't be revealed, as it belongs to the industry partner.

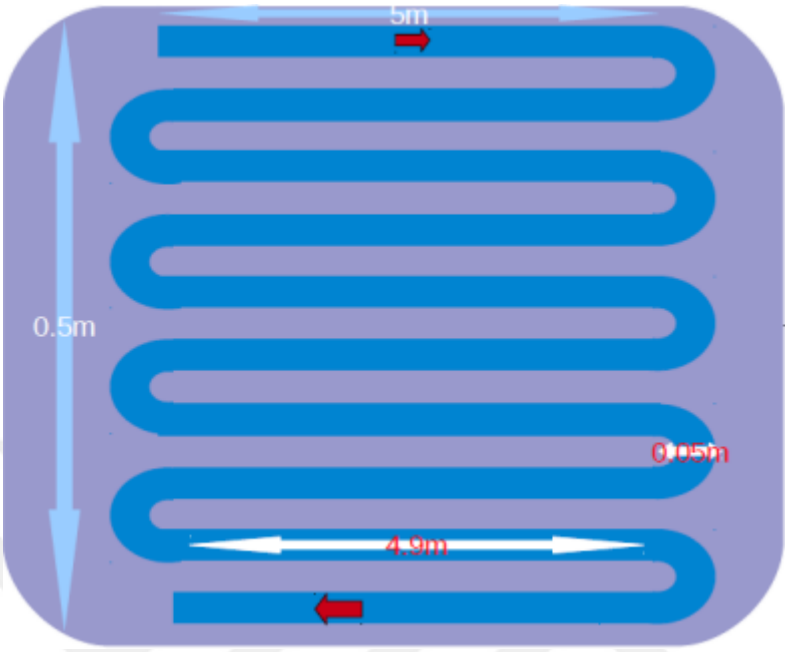

Figure 3.4: Scheme of An Evaporator Loop for the Geometry.

3.6 MODELING PHYSICAL PHENOMENA

In order to best model the thermo-hydraulic phenomena, we have used different diphasic models. Due to the results of the preliminary studies, the inlet flow of the evaporator is assumed to be annular with the gas circulating in the middle of the pipe and the liquid lying at the level of the wall. The heat emitted by the electronic components will cause the liquid to change phase. The steam title will grow, and the surface speed of the gas will increase. Due to the difference in speed between gas and liquid, there is going to be a tearing of liquid droplets at the interface between the two phases from a critical velocity. From a study carried out previously, we could see that the grubbing-up had no effect on the flow. This is surely because the number of droplets pulling out is low vis-à-vis the annular flow. Thus, we decided not to model this phenomenon of grubbing because of its negligible weight. From a purely thermal point of view, we place ourselves in a saturated boiling regime and model the heat exchange coefficient . When the title of the vapor phase is important enough to consider that the flow is monophasic, we use the monophasic thermal model. We modeled the interfacial frictions with the Wallis and parietal friction with the models. We will also note

that a singular load loss model at the elbows (valid in no gravity) has been implemented. From our various studies, we have found that the homogeneous model should be used for weaker titles, than the ones we are studying. Indeed, we find that the velocity changes are increasingly weak when the steam title is also. Finally, when the steam title is unitary, we use a monophasic model.

3.6.1 Hydraulic Models

Annular model without tearing: When the gas flow is important, the forces of gravity are highly negligible in front of the inertia forces. The liquid then completely moistens the wall by forming an annular film around the gas flow. The flow remains at separate phases. In addition, at very high gas flow drops of liquid are torn off and driven by the gas phase. This flow is said to be annular to droplets (annular dispersed). The annular model without tearing [1] Consists of two equations of movement quantity as well as the equation of conservation of the enthalpy. This system allows us to determine the pressure gradient, the evolution of the void rate as well as the title of the coolant fluid. Movement Quantity Conservation equations are below:

$$\frac{dR_g}{da} G^2 \left(\frac{R_l x^2}{\rho_g R_g^2} + \frac{R_g(1-x)^2}{\rho_l R_l^2}\right) = -\frac{c_{ig}4}{D}\sqrt{\overline{Rg}} + R_g \frac{c_{ig}4}{D} - (\rho_l - \rho_g) R_g R_l g + G^2 \frac{dx}{dz}\left(\frac{2xR_l}{\rho_g R_g} + \frac{(1-x)(2R_g-1)}{\rho_l R_l}\right) \quad (3.1)$$

$$\frac{dp}{dz} = -\frac{d}{dz}\left(\frac{G^2 x^2}{\rho_g R_g}\right) - \frac{d}{dz}\left(\frac{G^2(1-x)^2}{\rho_l R_l}\right) + \frac{c_p 4}{D} - (\rho_l R_l + \rho_g R_g) g \quad (3.2)$$

Equations for the conservation of enthalpy are below:

$$\frac{dy}{dz} = \frac{4q}{GDh_{tv}} \quad (3.3)$$

$$\delta = 0.5D(1 - \sqrt{R_g}) \quad (3.4)$$

These equations are used when the refrigerant is at a component level. When this is not the case, we consider the constant vacuum rate, as well as the title (there is no heat exchange). The terms of derivatives in the right-hand member of Equation 2 are then null, which also simplifies its expression.

Homogeneous model: The Homogeneous model [1] is valid in the context of dispersed flows with low speed of sliding of the gas relative to the liquid. This model assumes that the gas velocity is equal to the speed of the liquid either Ul= Ing= InM. In our configuration, we do not use the homogeneous model because the equal velocity hypothesis tends to be validated when the steam title is in a lower range than the one we are studying. We put it in this report, only for an informative purpose. The hypothesis that Ul = Ing = InM gives us 2 equations that allow the simplification of the model.

$$\rho_M = R_g\,\rho_g + (1 - R_g)\rho t \qquad et \qquad \frac{Gx}{\rho_g R_g} = \frac{G(1-x)}{\rho_l(1-R_g)} \tag{3.5}$$

The other equations to be computed also correspond to a movement quantity conservation equation and a pressure-resolution equation.

$$\frac{\mathrm{P}\rho_M U_M}{\mathrm{P}t} + \frac{\mathrm{P}}{\mathrm{P}z}\left[\rho_M U_M^2\right] = \frac{\mathrm{P}G}{\mathrm{P}t} + \frac{\mathrm{P}}{\mathrm{P}z}\left[\frac{G}{\rho_M}\right] = -\frac{dp}{dz} + \frac{c_p S_p}{A} - \rho M g sin\theta \tag{3.6}$$

$$\left(\frac{dp}{dz}\right)_{fr} = \frac{c_p S_p}{A} = \frac{S_p}{A}\frac{1}{2} f_{pM}\frac{G^2}{\rho M} = -\frac{S_p}{A}\frac{1}{2} f_{pM}\rho M U_M^2 \tag{3.7}$$

The coefficient fpm corresponds to the coefficient of skin friction. It is determined according to the value of the average Reynolds, noted ReM. On a $ReM = GD\ \mu M$ The value of the average viscosity μM is given by $\mu M = Rg\mu g + (1 - Rg)\mu$l

Monophasic model: When the steam title reaches the unit, we then use the Monophasic model [1]. Our specifications imposing on output, a mass title of 1 at the level of the vapor phase, it is normal that we are interested, in a one fluid model to calculate the pressure loss.

$$\frac{dp}{dz} = \frac{4c_\rho}{D} \tag{3.8}$$

With $rp = -0.5c * {}_g f\ \rho U2$

3.6.2 Model Complements

Wallis model: The Wallis model allows us to model the interfacial friction *i* between the liquid phase and the gas phase. We have the following system of equations:

$$r_i = -\frac{1}{2} f_i \rho_g |U_g - U_l| \tag{3.9}$$

$$f_i = 0.005\,(1 + 300\frac{\delta}{D}) = 0.005[1 + 150(1 - \sqrt{R_g})] \tag{3.10}$$

The gas and liquid velocities are determined from the surface velocities calculated at each step of space.

Lockhart and Martinelli model: The Lockhart and Martinelli model [1] allow to determine the skin friction at the level of our system. At the level of this model, we must calculate the parameter C first. This parameter is necessary for us to calculate the pressure loss. The Coefficients of wall friction are defined in the following way:

$$f_{pl} = K\,(\frac{JlD}{V_l})^{-n} \tag{3.11}$$

$$f_{pg} = K\,(\frac{JgD}{V_g})^{-n} \tag{3.12}$$

In laminar flow n = 1, k = 16 and in turbulent flow n = 1/4, k = 0.079.

In order to calculate the parameter C, we must first look at the flow regime in which we are located, both at the gas level and the liquid. So, we need to know the values of the Re. The following table shows the value of parameter C based on flow regimes.

Table 3.1: The Value of Parameter C Based on Flow Regimes.

Liquid	**Gas**	**C**
Turbulent	Turbulent	20
Laminar	Turbulent	12
Turbulent	Laminar	10
Laminar	Laminar	5

The Laminar regime is Defined for a Reynolds less than 2000 and the turbulent regime for a Reynolds greater than 3000. So, there is no correlation in the transition zone. In our simulations, the regime change caused discontinuities in the expression of the diphasic friction constraint. The problem was solved using the smoothing proposed by Julien Hugon. This linear interpolation of C is a function of log (Rel) and/or log (Reg). When only one of the two phases are in the transition zone (most frequently encountered), linear interpolation of C is Type C (rel) = a * log (rel) + B or C (reg) = a ' * log (reg) + B '. For example, in the case where the gas is in turbulent conditions and the liquid is in transition, the correlation used is:

$$C(Re_l) = \frac{20-12}{\log(3000)-\log(2000)} * (log(Re_l) - log(2000)) + 12 \quad (3.13)$$

In the case where the two phases are in transition zones, two linear C-interpolations of type C (rel, REG) = A * log (rel) + b * Log (REG) + C are used, one for rel > Reg and the other for rel < Reg.

Baroczy model: The Baroczy correlation [4] expresses the loss of pressure by diphasic friction depending on the friction loss (DP/DZ), that one would have if the liquid phase flowed alone with the same mass flow rate as the diphasic flow, $\dot{m}$. For this, it is necessary to be able to express the multiplicative coefficient $\varphi l0$ defined in the following way:

$$\varphi_{l0}^2 = \frac{(\frac{dp}{dz})_{fr}}{(\frac{dp}{dz})_l} \quad (3.14)$$

The two phases flowing alone, with the same mass flow as the diphasic flow, would have respectively the average velocities $Vl = G/\rho l$ And $Vg = G/\rho g$, from which we can define Reynolds numbers $Revl$ And $Revg$

Baroczy gives an expression of $\varphi l0$, from many experimental points grouping different fluids. The correlation obtained is graphic, but its curves were subsequently correlated by Chisholm in 1973, which obtained the following expression:

$$\varphi_{l0}^2 = 1 + (Y^2 - 1)[Bx^{\frac{2-n}{2}}(1-x)^{\frac{2-n}{2}} + x^{2-n}] \quad (3.15)$$

n is the opposite of the exponent of $Revl$ That we have in F ($Revl$), or n = 1 if the liquid flow alone is laminar ($Revl$ < 2000) and n = 0.25 If it is turbulent ($Revl$ > 3000). For the transition zone, the same value is used in the model as in the turbulent case, i.e. N = 0.25. B is a Y-and G-dependent variable whose expression varies depending on the value of y:

Y value	0 < and < 9.5	9.5≤and < 28	28≤Y
Value of B	$\frac{55}{G^{1/2}}$	$\frac{520}{YG^{1/2}}$	$\frac{1500}{Y^2G^{1/2}}$

Finally, the pressure losses can be calculated by friction:

$$\left(\frac{dp}{dz}\right)_{fr} = \varphi_{l0}^{2}\left(\frac{dp}{dz}\right)_{l} \tag{3.16}$$

Model of pressure loss in the elbows: In the literature, we have determined the empirical model suitable for load losses [3]. Δprb corresponds to the total load loss in the elbow for a diphasic flow:

$$\Delta P_{rb} = \emptyset \Delta P_{sp} \tag{3.17}$$

With Δpsp, total loss of load in the elbow in monophasic situation, expressed in the following manner:

$$\Delta P_{sp} = K_{sp}\frac{G^2}{2\rho_l} \tag{3.18}$$

3.6.3 Thermal Models

At the level of our geometry, we know all the constant fluxes released by the electronic components. This heat created is of course dissipated by the vaporization of the fluid circulating within the evaporator. Our goal is to determine the temperature of the different components. For this, we consider that the fluid enters the evaporator at its Tsat saturation temperature. The entire heat flux will be used to vaporize the refrigerant. Locally, a thermal balance gives us:

$$G * C_p * dT = q\pi D dz \tag{3.19}$$

For each step of space, we then obtain the value of the temperature at the wall of our evaporator. Furthermore, it is assumed that when a state change occurs at the fluid level, the vapor and liquid phases are in thermodynamic equilibrium. It is then possible to access the evolution of the mass title along the evaporator:

$$\frac{dx}{dz} = \frac{4*q}{m*h_{lv}*D} \tag{3.20}$$

Now that we know the evolution of the temperature of the wall of our evaporator, we are able to determine the evolution of the temperature of the different components. Indeed, a "circuit" of thermal resistances allows to connect these 2 temperatures. At the level of our geometry, the cylindrical tubes are attached to fins. These fins are in contact with the components in question. Our components, as previously said, are considered to be imitators that dissipate energy in a homogeneous way. The different resistances considered are:

i. A convection resistance at the level of the fluid/wall exchange, determined by heat exchange coefficient models.

ii. A conduction resistance between the wall of the tubes and the fins. As this resistance has not yet been determined.

iii. A contact resistance between the sole of the evaporator and the copycat which is 2e-4 K. m2 /w.

Below, the figure shows us a pattern of thermal resistances. This pattern is right there with a representative character. Indeed, some components include 9 tubes (3 * 3 tubes), and in this case the direction of flow is not the same in the different tubes covered by the component (change of the sign of gravity)

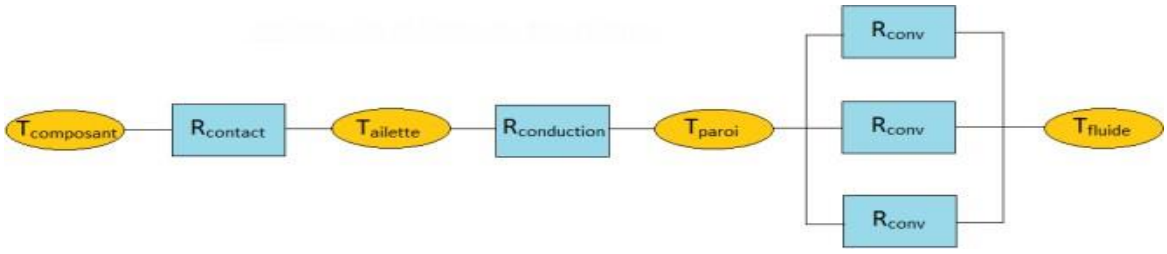

Figure 3.5: Schema of Thermic Resistance.

We can nevertheless from the previous figure find how to calculate our component temperature from that of the fluid, all other quantities being known.

In the case where the liquid film has a laminar flow (Rel < 2000), the wall temperature can be calculated from a conductive model. The following equation is obtained:

$$q_p = h_l \frac{T_p - T_{sat}}{\delta} \tag{3.20}$$

With δ the thickness of the film and kl the thermal conductivity of the fluid.

At the convective exchange rate, we decided to test the several models at our disposal applying to the saturated boiling regime. Indeed, this regime is the one that is correlated with the annular regime, from a thermal point of view. Since in the evaporator, the bulk of the fluid will be in this form there in diphasic, it makes sense to be interested in these different models. When the mass Title X 1, we know we're getting closer to a monophasic situation. At this time, of course, a monophasic model is used for the thermal aspect. In all models that will follow, the mass title is always calculated by the following enthalpy balance:

$$x(Z) = \frac{4q_p}{DGh_{lg}} (Z - Z_s) \tag{3.21}$$

In our case of study, the heating is carried out at imposed flux q. In order to know Tp, we will have to first calculate the value of hl.

4. RESULT AND DISCUSSION

Our MATLAB program consists of a main program that is responsible for calling the other scripts and consolidating the results. First, this one imports the geometry and the data of the refrigerant in order to be able to initialize the remainder of the program. The geometry has been divided into several parts: presence or not of a component, elbow. Each party has its own specifics. Once this data is retrieved, we initialize a first program that solves the equations for the vacuum rate, the title, and the pressure. The latter defines which model to use (annular or monophasic model) according to the previous results. Once these equations are resolved over all geometry, the program calls the scripts that calculate the temperature of the components, one script per model. These data, as well as the previous ones, are subsequently drawn up and grouped in order to be exploited. The simulations to determine the different parameters were carried out for two cases: with and without gravity. We can compare the different results obtained. In addition, to simplify the resolution, we have calculated these parameters for only one single tube.

Figure 4.1: Evolution of Quality in Tubing.

This first curve allows us to check the evolution of the title along the evaporator. One of the conditions of good functioning of it, is the disappearance of the liquid phase in its exit. In fact, this steam will then be overheated before radiating into space. If liquid is still present, the compressor will not be able to function properly. Here, for both cases, the refrigerant is totally in the form of vapor at the end. The condition is filled.

In the program, the condition x = 1 has been replaced by x = 0.99: some equations contain 1/(1-X) factor, which can lead to different problems of continuity and validity of the models. Beyond 0.99, we consider the constant title (the liquid phase is negligible). The increase of the title corresponds here to the passage of the tube at the level of a component because the evolution of the title means that the fluid moves from the liquid phase to that of steam. Now that we have looked at the evolution of the title, it may be interesting to compare it to that of the void rate.

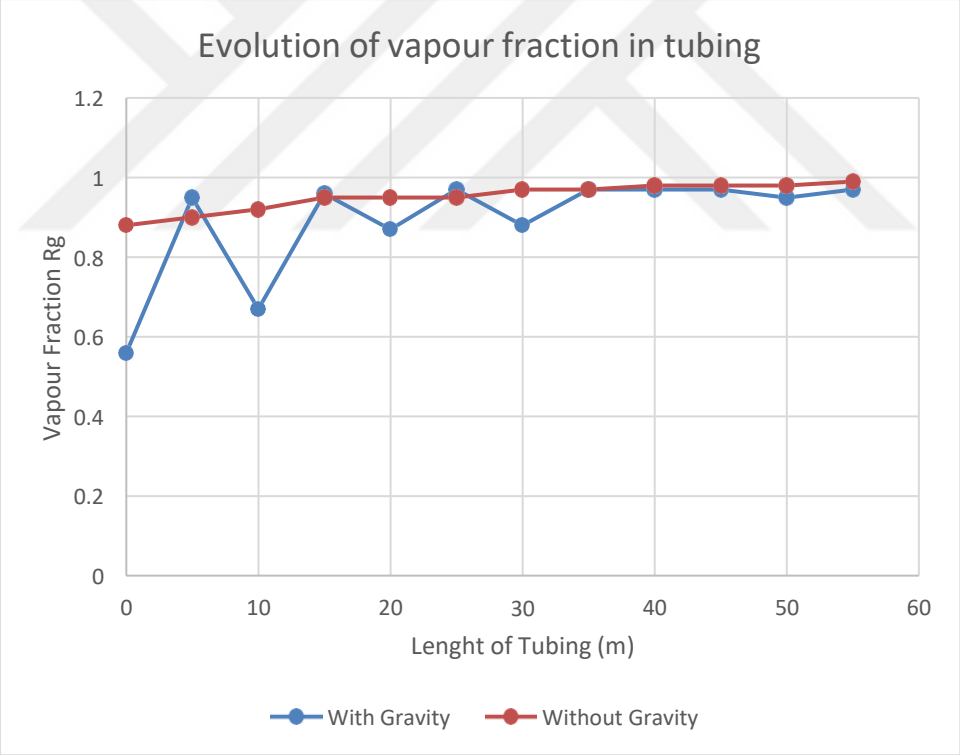

Figure 4.2: Evolution of Vapor Fraction in Tubing.

As before, the vacuum rate is limited to 0.99 to avoid different problems. The whole flow will be considered as monophasic beyond. In addition, both cases have well reached the limit of 1 at the end of the evaporator. The difference between the two cases here is blatant. Indeed,

gravity strongly influences the flow in the tubes, especially the liquid phase. The latter is accelerated in the downward tubes and slowed down in the ascending tubes. Because of flow retention, this causes a change in the thickness of the liquid layer, and therefore of the rate Rl: An increase for the ascending tubes, and a decrease for those descendants. So it is normal that all this influences the void rate: Rg = 1 - Rl . It is therefore normal that the curve without gravity is ‘smoother ‘, as it is only influenced by the presence of components. This alternation due to gravity can be observed in the velocities of the two phases.

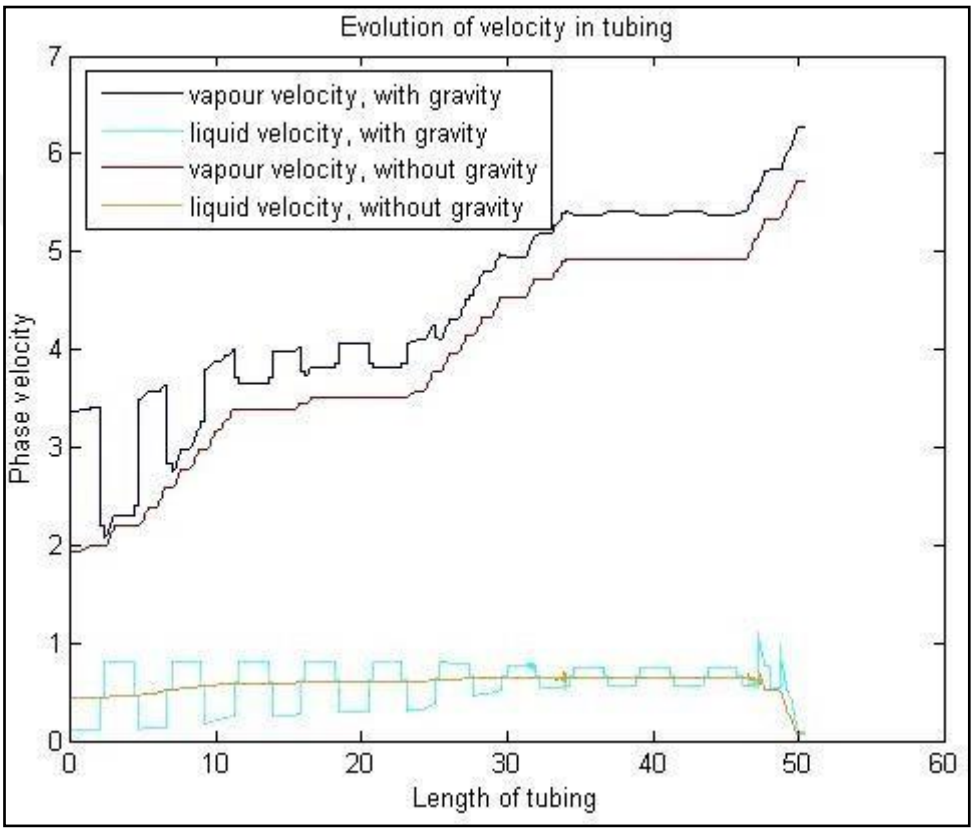

Figure 4.3: Evolution of Velocity in Tubing

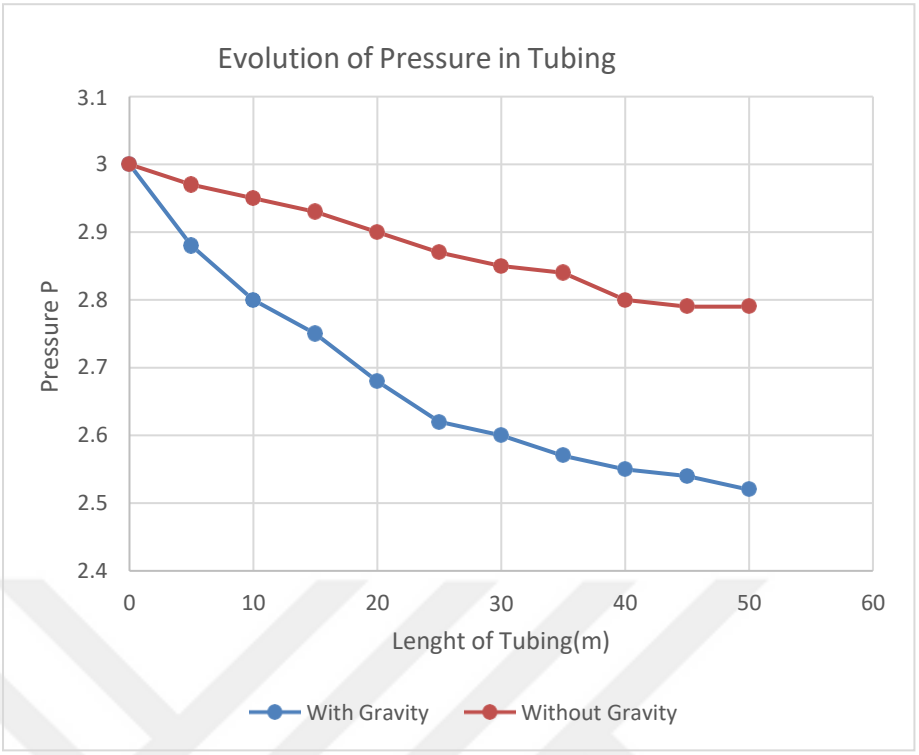

Figure 4.4: Evolution of Pressure in Tubing

Just like the previous data, the pressure inside the tubes is essential in order to calculate correctly the temperature of the components we must cool.

Pressure loss is an important part of our system. Indeed, the refrigerant remains at saturation temperature, even when the pressure changes: if it decreases, the temperature also decreases. However, the difference between the entry and the output for the latter shall not exceed 1 °C. So, we tried to take into account a number of phenomena to be as close to reality as possible. The evolution of pressure on this curve therefore includes the pressure loss in the elbows.

Here, the pressure losses correspond to a temperature drop of 5 °C with gravity, and 2 °C without. This difference is explained with additional pressure losses, due to the friction of the liquid caused by gravity. When switching to the monophasic case, we neglect the gas pressure loss. The same phenomenon can be observed in the case with gravity: bearings are present, corresponding to an ascending tube, or a downward tube. The temperature was

calculated for the three models:. These results allow us to clearly analyze the influence (and its absence) of gravity on the system.

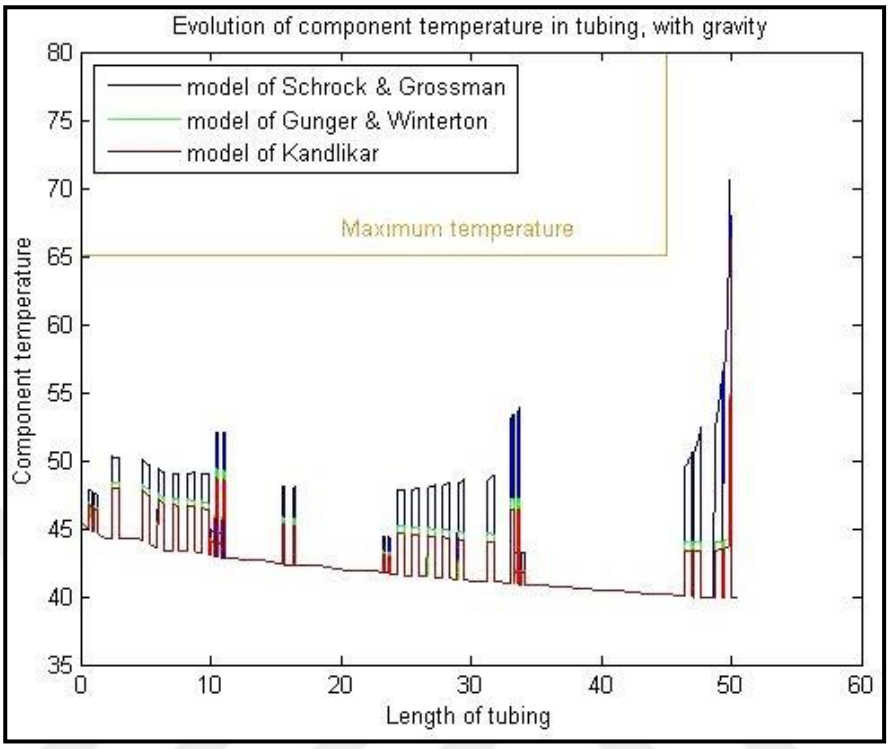

Figure 4.5: Evolution of Component Temperature in Tubing With Gravity.

The maximum temperature of the components has been added in order to better situate any problems. Overall, the components do not reach their critical temperature. However, locally, at the end of the evaporator, in the case without gravity, the temperature can reach 90 °C (instead of the 80 °C supported). This phenomenon is explained by the limit we have taken for the vacuum rate and the title. This definition eventually leads to the beginning of the monophasic zone, and thus to model changes, including for temperature. This is equivalent to heating up the gas temperature locally earlier, and therefore longer, instead of evaporating the little liquid that remains.

In addition, at high vacuum rates, the models used are less effective at predicting heat transfer. By pushing the limit and refining the models, we will arrive at the best prediction of this last temperature. The various simulations allow us to check the proper functioning of such an evaporator. All that remains is to confirm the theory with ground tests and compare the different points. Particular attention may be given to the last components of the system to check that the temperature limit is not reached.

4.1 CONCLUSION

In the framework this work, we have set up a framework to model the thermo-hydraulic phenomena in the evaporator of the cooling circuit of a satellite. Studies have taken into account the transition between different models as the flow regime changes in the evaporator. We compared the influence of different models at the level of interfacial friction and thermal. The studies also focused on respect for the geometry provided by the industrial partner. Our modelling of the system is in accordance with the specifications. Indeed, whether at the level of the pressure losses or for the maximum temperature of the components, the various simulations we have carried out are in accordance with the requirements. Nevertheless, some aspects dealt with in this project can be deepened in further studies. The study of other physical models such as the annular, with consider of the grubbing could be carried out. At thermal level Chen's model could also be tested. In addition, we missed for this study the experimental data that would have allowed us to make a coherent comparison.

5. CONCLUSION AND FUTURE WORKS

5.1 CONCLUSION

The experimental campaign allowed for the collection of usable data to define the behavior of the system under various operating settings and to identify the most crucial parameters on which to intervene to improve performance. The evaporator, on which this analysis is based, has performed admirably, particularly in terms of pressure losses, which have been almost non-existent. Thermal insulation proved to be the most significant element, as considerable heat loss values with the environment were observed in all tests. However, it should be noted that the experimental research was severely constrained by the electrical resistance anomaly, and that many features, as a result, require further investigation at higher powers. For instance, the volume of fluid inside the evaporator has changed enormously, moving toward the greatest worth on various events, especially when high stream and electrical power values were applied. The outcomes uncovered that it is controlled by a mind boggling balance dependent on various boundaries, making an authoritative end hard to figure out. Likewise, when the presence of an expander was mimicked, the ideal proficiency results were accomplished at the center force of 6 kW, with a continuous debasement for higher powers. Concerning the evaporator packing, it has been resolved that it is hard to make the framework work under various power loads without a gadget, for example, a beneficiary fit for putting away piece of the refrigerating liquid available for use and hence keeping away from lopsided characteristics in the heap of the condenser and evaporator. The elective methodology proposed is to assess the plan of the evaporator by offering an augmentation of the tank situated in the upper half. The tension proportion, which characterizes the distinction in enthalpy between the info and result of the expander, has had the best impact on the cycle's effectiveness. In light of the requirements forced (most strikingly on temperature), it has not forever been imaginable to expand the strain at the evaporator yield with expanding power, nor has it forever been feasible to keep up with the tension at the condenser input at consistent and low qualities. This brought about a fall in the strain proportion and, subsequently, in the cycle's thermodynamic effectiveness. Given these worries, it is obvious that extra testing at more prominent powers are expected to substantiate the speculation and gather a bigger data set of data.

5.2 FUTURE WORKS

Nonetheless, the writer accepts that few plant constraints are as of now clear and that a few medicines can be completed prior to pushing ahead with another exploratory mission, both to increment execution and to empower information gathering. These improvements are summed up underneath:

i. Accurately protect the evaporator to lessen heat trades with the climate.

ii. After the condenser, introduce a fluid collector to kill unnecessary fluid burdens in the evaporator.

iii. Robotize the assortment of information on refrigerant mass stream rate and fluid level inside the evaporator.

iv. Give an inverter control to consequently balance the rotational speed of the siphon until framework adjustment is accomplished.

One of the most fascinating potential outcomes is to make an evaporator model by altering the thermosyphon model displayed in Part 2. This will permit reproductions to happen beyond the working settings of the seat test, extrapolating results for bigger powers and giving more data on the chance of utilizing this innovation in modern applications. It will likewise be more straightforward to distinguish misfortune causes and to completely analyze as far as possible connected with the two-stage shut thermosyphon innovation. A first methodology has been taken in this exposition to assess the suitability of utilizing a thermosyphon heat exchanger for squander heat recuperation. The improved on model that was tried yielded empowering results, especially as far as the essential perspectives associated with the particular shape and the functioning rule that depends on gravity to recycle liquid. Numerous components of this examination require more examination, yet the innovation has demonstrated potential for future upgrades in the field of modern waste intensity recuperation utilizing ORC frameworks.

REFERENCES

[1] NASA, 'NASA Technology Roadmaps TA 14 : Thermal Management Systems', 2015.

[2] C. Nadjahi, H. Louahlia, and S. Lemasson, 'Sustainable Computing : Informatics and Systems', Sustain. Comput. Informatics Syst., vol. 19, no. May, pp. 14–28, 2018.

[3] S. Khandekar and M. Groll, 'On the definition of pulsating heat pipes: an overview', in 5th Heat Pipes, Heat Pumps and Refrigerators International Seminar , Minsk, 2003, vol. 3.

[4] D. Reay and P. Kew, Heat Pipes: theory, design and applications, 5th ed. Oxford: Butterworth-Heinemann, 2006.

[5] M. S. El-Genk and H. H. Saber, 'Heat Transfer Correlations for Liquid Film in the Evaporator of Enclosed, Gravity-Assisted Thermosyphons', vol. 120, no. 2, 1998.

[6] F. Zhou, G. Ma, Z. Liu, F. Li, and X. Yan, 'Heat transfer characteristics of thermosyphon heat exchanger for cooling electrical cabinet', pp. 1–7, 2018.

[7] H. Jouhara and A. J. Robinson, 'Experimental investigation of small diameter two-phase closed thermosyphons charged with water , FC-84 , FC-77 and FC3283', Appl. Therm. Eng., vol. 30, no. 2–3, pp. 201–211, 2010.

[8] D. Jafari, A. Franco, S. Filippeschi, and P. Di Marco, 'Two-phase closed thermosyphons : A review of studies and solar applications', vol. 53, pp. 575– 593, 2016.

[9] A. Franco and S. Filippeschi, 'Closed loop two-phase thermosyphon of small dimensions: A review of the experimental results', Microgravity Sci. Technol., vol. 24, no. 3, pp. 165–179, 2012.

[10] J. M. Ochterbeck, 'Heat Pipes', in Heat transfer handbook, A. Bejan and A. D. Kraus, Eds. John Wiley & Sons, 2003, pp. 1181–1230.

[11] Y. F. Maidanik and Y. G. Fershtater, 'Theoretical Basis and Classification ofLoop Heat Pipes and Capillary Pumped Loops', in Proc. 10th International Heat Pipe Conference, 1997

[12] Liu, J.; Guo, K.H.; He, Z.H.; Li, T.X. Start-up investigation on a dual-evaporator MPCL system. Exp. Therm. Fluid Sci. 2009, 33, 555–560.

[13] Zhang, Z.; Sun, X.H.; Tong, G.N.; Huang, Z.-C.; He, Z.-H.; Pauw, A.; van Es, J.; Battiston, R.; Borsini, S.; Laudi, S.; et al. Stable and self-adaptive performance of mechanically pumped CO2 two-phase loops for AMS-02 tracker thermal control in vacuum. Appl. Therm. Eng. 2011, 31, 3783–3791.

[14] Meng, Q.L.; Zhang, T.; Yu, F.; ZY, Y.; Zhao, Z.; Zhou, Z. Experimental study on the dynamic behavior of mechanically pumped two-phase loop with a novel accumulator in the simulated space environment. Chin. J. Aeronaut. 2022, in press.

[15] Delil, A.A.M., Fundamental Differences between Liquid-Vapour and Liquid-Gas Two-Phase Flow and Heat Transfer, Keynote Lecture, Proc. 5th Int. Seminar on Heat Pipes, Heat Pumps and Refrigerators, Minsk, Belarus, 2003

[16] Zhang, C.B.; Li, G.R.; Sun, L.; Chen, Y.P. Experimental study on active disturbance rejection temperature control of a mechanically pumped two-phase loop. Int. J. Refrig. 2021, 129, 1–10.

[17] Delil, A.A.M., Two-Phase Heat Transport Systems for Space: Thermal Gravitational Modelling & Scaling, Similarity Considerations, Equations, Predictions, Experimental Data and Flow Pattern Mapping, Proc. CPL '98 International Workshop, El Segundo, USA, 2-3 March 1998.

[18] Gerner, H.J. Transient Modelling of Pumped Two-Phase Cooling Systems: Comparison between Experiment and Simulation. In Proceedings of the 46th International Conference on Environmental Systems, Vienna, Austria, 10 June–14 July 2016.

[19] Gerner, H.J.; Bolder, R.; van Es, J. Transient modelling of pumped two-phase cooling systems: Comparison between experiment and simulation with R134a. In Proceedings of the 47th International Conference on Environmental Systems, Charleston, SC, USA, 16–20 July 2017.

[20] Khalil, U.R.; Wasfi, S.; Kamaleldin, A. A group theoretic analysis on heat transfer in MHD thermally slip Carreau fluid subject to multiple flow regimes (MFRs). Case Stud. Therm. Eng. 2022, 30, 101787.

[21] M. Naidu, T. W. Nehl, S. Gopalakrishnan, and L. Würth, “Electric Compressor Drive with Integrated Electronics for 42 V Automotive HVAC Systems,” presented at the SAE 2005 World Congress & Exhibition, 2005.

[22] R. Baumgart, J. Aurich, J. Ackermann, and C. Danzer, “Comparison and Evaluation of a New Innovative Drive Concept for the Air Conditioning Compressor of Electric Vehicles,” SAE International, Warrendale, PA, 2015-26–0045, Jan. 2015.

[23] M. Wei, H. Huang, P. Song, F. Peng, Z. Wang, and H. Zhang, “Experimental investigations of different compressors based electric vehicle heat pump air-conditioning systems in low temperature environment,” in 2014 IEEE Conference and Expo Transportation Electrification Asia-Pacific (ITEC Asia-Pacific), Beijing, China, 2014, pp. 1–6.

[24] D. Krahenbuhl, C. Zwyssig, H. Weser, and J. W. Kolar, “A Miniature 500 000-r/min Electrically Driven Turbocompressor,” IEEE Trans. Ind. Appl., vol. 46, no. 6, pp. 2459–2466, Nov. 2010.

[25] R. W. Cummings and R. K. Shah, “Experimental Performance Evaluation of Automotive AirConditioning Heat Exchangers as Components and in Vehicle Systems,” presented at the Vehicle Thermal Management Systems Conference & Exposition, 2005.

[26] Y. Han, Y. Liu, M. Li, and J. Huang, “A review of development of micro-channel heat exchanger applied in air-conditioning system,” Energy Procedia, vol. 14, pp. 148–153, 2012.

[27] Z. Qi, Y. Zhao, and J. Chen, “Performance enhancement study of mobile air conditioning system using microchannel heat exchangers,” Int. J. Refrig., vol. 33, no. 2, pp. 301–312, Mar. 2010.

[28] J. H. Ahn, J. S. Lee, C. Baek, and Y. Kim, “Performance improvement of a dehumidifying heat pump using an additional waste heat source in electric vehicles with low occupancy,” Energy, vol. 115, pp. 67–75, Nov. 2016.

[29] C. Kwon, M. S. Kim, Y. Choi, and M. S. Kim, “Performance evaluation of a vapor injection heat pump system for electric vehicles,” Int. J. Refrig., vol. 74, pp. 138–150, Feb. 2017.

[30] C. Kowsky, L. Leitzel, F. Oddi, and E. Wolfe, “Unitary HPAC System - Commercial Vehicle Applications,” presented at the SAE 2012 Commercial Vehicle Engineering Congress, 2012.

[31] V. Pommé, “Reversible Heat Pump System for an Electrical Vehicle,” presented at the 1995 Vehicle Thermal Management Systems Conference and Exhibition, 1997.

[32] J. H. Ahn, H. Kang, H. S. Lee, H. W. Jung, C. Baek, and Y. Kim, “Heating performance characteristics of a dual source heat pump using air and waste heat in electric vehicles,” Appl. Energy, vol. 119, pp. 1–9, Apr. 2014.

[33] J. H. Ahn, H. Kang, H. S. Lee, and Y. Kim, “Performance characteristics of a dual-evaporator heat pump system for effective dehumidifying and heating of a cabin in electric vehicles,” Appl. Energy, vol. 146, pp. 29–37, May 2015.

[34] D. Wang, T. Gao, W. Li, Y. Yang, J. Shi, and J. Chen, “System Characteristics of Direct and Secondary Loop Heat Pump for Electrical Vehicles,” presented at the WCX World Congress Experience, 2018.

[35] S. Bilodeau, “High Performance Climate Control for Alternative Fuel Vehicle,” presented at the 1995 Vehicle Thermal Management Systems Conference and Exhibition, 2001.

[36] D. Antonijevic and R. Heckt, “Heat pump supplemental heating system for motor vehicles,” Proc. Inst. Mech. Eng. Part J. Automob. Eng., vol. 218, no. 10, pp. 1111–1115, Oct. 2004.

[37] J. M. Calm, “The next generation of refrigerants – Historical review, considerations, and outlook,” Int. J. Refrig., vol. 31, no. 7, pp. 1123–1133, Nov. 2008.

[38] European Parliament, “Regulation (EC) No. 842/2006 of the European Parliament and of the council of 17 May 2006 on certain fluorinated greenhouse gases,” Official Journal of the European Union, vol. L161, p. 11, Jun. 206AD.

[39] R. Mcenaney and P. Hrnjak, “Clutch Cycling Mode of Compressor Capacity Control of Transcritical R744 Systems Compared to R134a Systems,” presented at the Vehicle Thermal Management Systems Conference & Exposition, 2005.

[40] M. Petersen, C. Bowers, S. Elbel, and P. Hrnjak, “Development of high-efficiency carbon dioxide commercial heat pump water heater,” HVACR Res., vol. 19, no. 7, pp. 823–835, Oct. 2013.

[41] Acharya, N., Sen, M., Chang, H. C., 2001. Analysis of Heat Transfer Enhancement in Coiled-tube Heat Exchangers. International Journal of Heat and Mass Transfer, Vol. 44, 44(1), pp. 102–108. https://doi.org/10.1016/S0017-9310(01)00002-3

[42] Akiyama, M., Cheng, K. C., 1972. Laminar Forced Convection Heat Transfer in Curved Pipes with Uniform Wall Temperature, International Journal of Heat and Mass Transfer, Vol. 15, pp. 1426-1431

[43] Dean, W. R., 1927. Note on the Motion of Fluid in a Curved Pipe. The London, Edinburgh, and Dublin Philosophical Magazine and Journal of Science Series 7 Vol. 4, 20. https://doi.org/10.1080/14786440708564324

[44] Dravid, A. N., Smith, K. A., Merrill, E. W., and Brian, P. L. T., 1971. Effect of Secondary Fluid Motion on Laminar Flow Heat Transfer in Helically Coiled Tubes. AIChE 17 (5): 1114–22. https://doi.org/10.1002/aic.690170517.

[45] Dubba, S. K., and Kumar, R., 2018. Experimental Investigation on Flow of R-600a Inside A Diabatic Helically Coiled Capillary Tube: Concentric Configuration. International Journal of Refrigeration. Elsevier Ltd, Vol. 45(4), 186–195. https://doi: 10.1016/j.ijrefrig.2017.10.035.

[46] Elazm, M. A., Ragheb, A., Elsafty, A., Teamah, M., 2012. Computational Analysis for the Effect of the Taper Angle and Helical Pitch on the Heat Transfer Characteristics of the Helical Cone Coils. The Archive of Mechanical Engineering, VOL. LIX, No. 3, 10.2478/V10180-012-0019-9.

[47] Elazm, M. A., Ragheb, A. M., Elsafty, A., Teamah, M. A., 2013. Numerical Investigation for the Heat Transfer Enhancement in Helical Cone Coils over Ordinary Helical Coils. Journal of Engineering Science and Technology, Vol.8, No.1, pp. 1–15.

[48] Flórez-orrego, D., Arias, W., Diego López, D., and Velásquez, H., 2012. Experimental and CFD Study of a Single-Phase Cone-Shaped Helical Coiled Heat Exchanger: An Empirical Correlation. Proceedings of Ecos -The 25th International Conference on Efficiency, Cost, Optimization, Simulation and Environmental Impact of Energy Systems, Vol. 375, 1–19.

[49] Ghorbani, N., Taherian, H., Gorji, M., Mirgolbabaei, H., 2010. Experimental study of mixed convection heat transfer in vertical helically coiled tube heat exchangers.. Experimental Thermal and Fluid Science, 34, 900–905. https://doi.org/10.1016/j.expthermflusci.2010 .02.004

[50] Guo, L., Feng, Z. P., and Chen, X., 2001. Transient Convective Heat Transfer of SteamWater Two-Phase Flow in a Helical Tube under Pressure Drop Type Oscillations. International Journal of Heat and Mass Transfer, 45 (3): 533–42. https://doi.org/10.1016/S0017-9310(01)00178-8.

[51] Haruki, N., Horibe, A., 2013. Flow and heat transfer characteristics of ice slurries in a helically-coiled pipe, International Journal of Refrigeration,36,1285-1293. https://doi.org/10.1016/j.ijrefrig.2013.02.010

[52] Hüttl, T. J., and Friedrich, R., 2000. Influence of Curvature and Torsion on Turbulent Flow in Helically Coiled Pipes. International Journal of Heat and Fluid Flow, 21 (3): 345–53. https://doi.org/10.1016/S0142-727X(00)00019-9.

[53] Imran, M., Tiwari, G., and Yadav, A., 2015. CFD Analysis of Heat Transfer Rate in Tube in Tube Helical Coil Heat Exchanger. International Journal of Innovative Science, Engineering & Technology, 2 (8): 53–57.

[54] Izadpanah, E., Zarei, A., Akhavan, S., Babaie, M. R., 2018. An Experimental Investigation of Natural Convection Heat Transfer from a Helically Coiled Heat Exchanger. International Journal of Refrigeration. Elsevier Ltd, 93, 38–46. https://doi: 10.1016/j.ijrefrig.2018.06.008.

[55] Jamshidi, N. and Mosaffa, A., 2018. Investigating the effects of geometric parameters on finned conical helical geothermal heat exchanger and its energy extraction capability. Geothermics, 76(May), 177–189. https://doi: 10.1016/j.geothermics.2018.07.007.

[56] Jayakumar, J. S., Mahajani, S. M., Mandal, J. C., Iyer, K. N., and Vijayan, P. K., 2010. CFD Analysis of Single-Phase Flows inside Helically Coiled Tubes. Computers and Chemical Engineering, 34 (4): 430–46. https://doi.org/10.1016/j.compchemeng. 2009.11.008.

[57] Jayakumar, J. S., Mahajani, S. M., Mandal, J. C., Vijayan, P. K., and Bhoi, R., 2008. Experimental and CFD Estimation of Heat Transfer in Helically Coiled Heat Exchangers. Chemical Engineering Research and Design, 86 (3): 221–32. https://doi.org/10.1016/j.cherd.2007.10.021.

[58] Joshi, S. M., Anand, S. R., 2015. Design of conical helical coil heat exchanger for waste heat recovery system, International Conference on Technologies for Sustainable Development (ICTSD-2015) Feb. 04 – 06, 2015, Mumbai, India

[59] Kannadasan, N., Ramanathan, K., Suresh, S., Comparison of heat transfer and pressure drop in horizontal and vertical helically coiled heat exchanger with

CuO/water based nano fluids, Experimental Thermal and Fluid Science, 42 (2012) 64–70.

[60] Kareem, R., 2017. Optimisation of Double Pipe Helical Tube Heat Exchanger and Its Comparison with Straight Double Tube Heat Exchanger. Journal of The Institution of Engineers (India): Series C, 98 (5): 587–93. https://doi.org/10.1007/s40032-016- 0261-x.

[61] Ke, Y.A.N., Pei-qi, G., Yan-cai, S., Hai-tao, M., 2011. Numerical Simulation on Heat Transfer Characteristic of Conical Spiral Tube Bundle. Applied Thermal Engineering 31 (2–3): 284–92. https://doi.org/10.1016/j.applthermaleng.2010.09.008

[62] Kuvadiya, M. N., Patel, R. A., Deshmukh, G. K., Bhoi, R. H., 2015. Parametric Analysis of Tube in Tube Helical Coil Heat Exchanger at Constant Wall Temperature. International Journal of Science Technology & Engineering, 1 (10): 279–85.

[63] Mahmoudi, M., Tavakoli, M. R., Mirsoleimani, M. A., Gholami, A., Salimpour, M. R., 2017. Experimental and numerical investigation on forced convection heat transfer and pressure drop in helically coiled pipes using TiO2/water nanofluid, International Journal of Refrigeration, 74,627-643. https://doi.org/10.1016/j.ijrefrig.2016.11.014

[64] Moawed, M., 2011. Experimental study of forced convection from helical coiled tubes with different parameters. Energy Convers. Manag. 52, 1150–1156. https://doi.org/ 10.1016/j.enconman.2010.09.009

[65] Naphon, P., and Suwagrai, J., 2007. Effect of curvature ratios on the heat transfer and flow developments in the horizontal spirally coiled tubes. International Journal of Heat and Mass Transfer, 50(3–4), 444–451. https://doi: 10.1016/j.ijheatmasstransfer .2006.08.002.

[66] Nobari, M. R. H., and Malvandi, A., 2013. Torsion and curvature effects on a fluid flow in a helical annulus, International Journal of Nonlinear Mechanics, 57, 90-101. https://doi.org/10.1016/j.ijnonlinmec.2013.06.014.

[67] Pimenta, T. A., and Campos, J. B. L. M., 2012. Friction losses of Newtonian and nonNewtonian fluids flowing in laminar regime in a helical coil. Experimental Thermal and Fluid Science. Elsevier Inc., 36, 194–204. https://doi: 10.1016/j.expthermflusci. 2011.09.013.

[68] Purandare, P. S., Lele, M. M., and Gupta, R.K., 2015. Experimental investigation on heat transfer analysis of conical coil heat exchanger with 90 cone angle. Heat Mass Transfer, 3, 373-379. https://doi 10.1007/s00231-014-1418-x.

[69] Purandare, P. S., Lele, M. M., Gupta, R. K., 2015. Investigation on thermal analysis of conical coil heat exchanger, International Journal of Heat and Mass Transfer, 90, 1188–1196. https://doi.org/10.1016/j.ijheatmasstransfer.2015.07.044

[70] Shokouhmand, H., and Salimpour, M. R., 2008. Experimental Investigation of Shell and Coiled Tube Heat Exchangers Using Wilson Plots. International Communications in Heat and Mass Transfer, 35 84–92 https://doi.org/10.1016/j.icheatmasstransfer.2 007.06.001.

[71] Xin, R. C., Awwad, A., Dong, Z. F., and Ebadian, M. A., 1997. An Experimental Study of Single-Phase and Two-Phase Flow Pressure Drop in Annular Helicoidal Pipes. International Journal of Heat and Fluid Flow, 18 (5): 482–88. https://doi.org/10.1016 /S0142-727X(97)80006-9

[72] Xu, X., Zhang, Y., Liu, C., Zhang, S., Dang, C.,2018. Experimental investigation of heat transfer of supercritical CO2 cooled in helically coiled tubes based on exergy analysis. International Journal of Refrigeration, 88, 177-185. https://doi.org/10.101 6/j.ijrefrig.2018.03.011.

[73] AI-Fahed, S. and Chakroun, W., (1996) Effect of tube tape clearance on heat transfer for fully developed turbulent flow in a horizontal isothermal tube, International Journal Heat and Fluid Flow, 17, 173–178.